Key Points:

- Scaling estimates of dissolved organic carbon (DOC) flux from the Onega River increases pan-Arctic DOC flux estimates by more than 50%
- Organic matter dynamics in the Onega River exhibit increased terrestrial signal and muted seasonality compared to the largest Arctic rivers
- Smaller watersheds must be included in Arctic DOC research for accurate models of pan-Arctic carbon dynamics

Supporting Information:

Supporting Information may be found in the online version of this article.

Correspondence to:
S. Starr,
sfs20bb@fsu.edu

Check for updates

AGU ADVANCING EARTH AND SPACE SCIENCE

Characterizing Uncertainty in Pan-Arctic Land-Ocean Dissolved Organic Carbon Flux: Insights From the Onega River, Russia

Sommer Starr[1], Sarah Ellen Johnston[1,2], Nikita Sobolev[3,4], Irina Perminova[4], Anne Kellerman[1], Greg Fiske[5], Ekaterina Bulygina[6], Alexander Shiklomanov[7], Amy McKenna[8,9], and Robert G. M. Spencer[1]

[1]National High Magnetic Field Laboratory Geochemistry Group, Department of Earth, Ocean, and Atmospheric Science, Florida State University, Tallahassee, FL, USA, [2]Department of Chemistry and Biochemistry, University of Alaska Fairbanks, Fairbanks, AK, USA, [3]Northern (Arctic) Federal University Named After M. V. Lomonosov, Arkhangelsk, Russia, [4]Department of Chemistry, Lomonosov Moscow State University, Moscow, Russia, [5]Woodwell Climate Research Center, Falmouth, MA, USA, [6]Louisiana Universities Marine Consortium, Chauvin, LA, USA, [7]Water Systems Analysis Group, University of New Hampshire, Durham, NH, USA, [8]National High Magnetic Field Laboratory FT-ICR MS Group, National High Magnetic Field Laboratory, Tallahassee, FL, USA, [9]Department of Soil and Crop Sciences, Colorado State University, Fort Collins, CO, USA

Abstract Dissolved organic carbon (DOC) flux from rivers in the pan-Arctic watershed represents an important connection between major terrestrial carbon stocks and the Arctic Ocean. Previous estimates of Arctic carbon flux and dissolved organic matter (DOM) seasonal dynamics have relied predominantly on measurements from the six major Arctic rivers, yet these may not be representative of northern high-latitude constrained smaller watersheds. Here, we evaluate DOC concentration and DOM composition in the Onega River, a small Arctic watershed, using optical measurements and ultrahigh resolution mass spectrometry. Compared to the six largest Arctic rivers, DOC, absorbance at a_{350}, and indicators of terrestrial DOM (e.g., specific UV absorbance at 254 nm, modified aromaticity index, relative abundance of condensed aromatics and polyphenolics) were elevated in the Onega throughout the year. Seasonality was also generally muted in comparison to the major Arctic rivers with relatively elevated DOC and terrestrial markers in both spring and fall seasons. The Onega exhibits a strong relationship between a_{350} and DOC, and its organic-rich nature is apparent in its high DOC yield (4.85 g m^{2}yr^{-1}), and higher chromophoric DOM per unit DOC than the six largest Arctic rivers. As DOC yield from the Onega may be more representative of smaller northern high-latitude rivers, we derived a new pan-Arctic DOC flux scaling estimate which is over 50% higher than previous estimates scaled solely from the six major Arctic rivers. These observations suggest that smaller northern high-latitude rivers may be underrepresented in Arctic carbon flux models and highlights uncertainty around constraining the export of DOC to the Arctic Ocean.

Plain Language Summary Arctic rivers export large amounts of carbon to the Arctic Ocean, but estimates of these carbon fluxes are historically limited by observations from only the largest rivers. Arctic carbon budgets that do not include smaller rivers may be underestimating the amount of carbon that moves from the land to the ocean due to different yields. We examined both the amount and form of carbon in the Onega River, a small river in the Arctic, by looking at water samples from different seasons to compare with the largest rivers that have been observed more often. Unlike in large rivers where the composition of carbon is strongly dependent on the season, the types of carbon present in the Onega River changed less between seasons and concentrations were higher year-round. The Onega River also had more carbon relative to its size than the largest six rivers (i.e., higher yield). We used the estimated flux from the Onega River and scaled it to other smaller watersheds across the Arctic and found that previous estimates on total carbon flux to the Arctic Ocean may be underestimated. This is important because more carbon being transported to the Arctic Ocean may produce more carbon dioxide with climate change feedbacks.

1. Introduction

Arctic and boreal soils contain approximately half of all global organic carbon (C), as many northern high-latitude landscapes are covered by C-rich permafrost and peatlands (Hugelius et al., 2014; Schuur et al., 2015; Tarnocai

et al., 2009). These C rich landscapes are connected to the Arctic Ocean via rivers, the six largest (Yenisey, Lena, Ob', Mackenzie, Yukon, and Kolyma) of which alone export an estimated 18.1 Tg yr^{-1} of dissolved organic carbon (DOC). Scaled to the entire pan-Arctic region, this results in an approximate DOC flux of 27.3 Tg yr^{-1} exported to the Arctic Ocean (Fabre et al., 2019; Holmes et al., 2012; Johnston et al., 2018; Raymond et al., 2007). These fluvial exports are a significant source of C and nutrients to the Arctic Ocean, and have been estimated to support as much as one third of total primary production in the Arctic Ocean (Terhaar et al., 2021). DOC exported from Arctic rivers and groundwater is so significant with respect to the Arctic Ocean that the entire basin has been described as having estuarine-like characteristics throughout (Connolly et al., 2020; McClelland et al., 2012). This export of C from Arctic soils and off the terrestrial landscape is of global importance, as a portion of Arctic Ocean DOC is subsequently exported to the global ocean where mineralization and gas exchange drives fluxes to the atmosphere (Amon et al., 2003; Kaiser et al., 2017; Kort et al., 2012). Additionally, northern high-latitude regions are warming more quickly than the global average, and this warming is predicted to impact DOC dynamics in Arctic rivers into the near future (Drake et al., 2015; Frey & Smith, 2005; Pokrovsky et al., 2020). Thus, accurately estimating the current flux of riverine DOC to the Arctic Ocean is fundamental to understanding the global C cycle now, and under future warming conditions.

Hydrologic conditions in Arctic rivers are highly seasonal, with even large rivers experiencing up to 60% of their annual discharge during the spring freshet, a two-to-four week window in the spring driven by snowmelt (Lammers et al., 2001; Mann et al., 2012; Spencer et al., 2008). The freshet brings with it not only elevated discharge, but also high concentrations of DOC combining to produce large fluxes during this short period of time (Holmes et al., 2012; Raymond et al., 2007; Spencer et al., 2009). The composition and thus fate of dissolved organic matter (DOM) transported by large Arctic rivers also varies dramatically across the seasons. During spring freshet, DOM is dominated by terrestrially sourced material and is highly aromatic in nature as evidenced by elevated specific UV absorbance at 254 nm (SUVA$_{254}$) values, lignin carbon-normalized yields, and high relative abundances of condensed aromatics and polyphenolics tied to allochthonous DOM inputs (Behnke et al., 2021; Mann et al., 2012; Spencer et al., 2008). Despite the dominance of a terrestrial signature during the freshet, DOM at this time of year has been shown to be highly biolabile due to a latent energy-rich spring subsidy as evidenced by a relatively higher proportion of high H/C formulas that are energetically favorable for microbial metabolism (Behnke et al., 2021; Holmes et al., 2008). At the opposite end of the spectrum to spring, winter riverine DOM transported under-ice tends to consist of lower molecular weight and less aromatic compounds with signatures of microbial origin (i.e., lower SUVA$_{254}$ and lignin carbon-normalized yields), and to be dominated by stable molecular formulae (Behnke et al., 2021; Mann et al., 2012; Spencer et al., 2009). As noted above in the largest Arctic rivers, the spring freshet comprises the majority of both discharge and DOC flux, but fall discharge events may be an important driver of DOC export in smaller watersheds. For example, northern high-latitude rivers across Eurasia display a second period of increased discharge in the fall, including the three watersheds that drain into the White Sea (the Onega, Severnaya Dvina, and Mezen), and the Tana and Pechora Rivers (Chupakov et al., 2020; Dankers & Middelkoop, 2007). Evidence from the Severnaya Dvina suggests that this second discharge event may also occur concurrent with increased DOC concentrations and thus elevated flux (Chupakov et al., 2020; Johnston et al., 2018), and may represent an important export and biogeochemical phenomenon that does not occur in the six largest Arctic rivers (i.e., the Ob', Yenisey, Lena, Kolyma, Yukon and Mackenzie Rivers).

Estimates of DOC flux to the Arctic Ocean are predominantly based on data collected from the six largest Arctic rivers, which make up 67% of the pan-Arctic watershed, defined as an area of 16.8×10^6 km^2 encompassing all catchments that drain into the Arctic Ocean and the Bering Sea, excluding northern Scandinavia and parts of Canada. This definition is the same as that used by the Arctic Great Rivers Observatory, where the pan-Arctic watershed includes all watersheds draining into the Arctic Ocean plus the Yukon River and rivers that drain into the Bering Sea (Holmes et al., 2012). The other ~33% of the pan-Arctic watershed area that drains into the Arctic Ocean is comprised of numerous small to medium-sized watersheds that represent understudied drainages that are constrained to northern high-latitudes (Holmes et al., 2013; Johnston et al., 2018). Historically, Arctic land-ocean DOC export estimates assumed that this unrepresented area (~33% of the pan-Arctic watershed) scaled linearly with the remaining two-thirds captured by the six largest Arctic rivers, and did not account for differences in land cover, permafrost extent, climate, and latitude. In addition, limited data from smaller northern high-latitude constrained rivers makes validating pan-Arctic DOC flux modeling difficult (Rawlins et al., 2021; Williamson et al., 2021), and previous research has shown that models based on the six largest Arctic rivers may

underestimate flux in comparison to the limited data that exists on smaller northern high-latitude constrained watersheds, as these smaller systems may have higher DOC yields (V. Gordeev et al., 1996; Johnston et al., 2018).

The origin and thus composition of riverine DOM is another important variable in understanding C cycling in the Arctic as this ultimately controls the material's fate and influences marine microbial metabolism, nutrient turnover, and primary production (Holmes et al., 2008; Mann et al., 2016; Terhaar et al., 2021). Therefore, it is critical to have an accurate understanding of DOM dynamics across the pan-Arctic watershed, including in the understudied northern high-latitude constrained riverine systems. Optical analysis of chromophoric DOM (CDOM) has been widely used to assess the source and composition of DOM in Arctic aquatic ecosystems (Mann et al., 2016; Pugach et al., 2018; Spencer et al., 2009) as it requires little sample volume, is analytically straightforward, and has the ability to even be undertaken in situ (Carstea et al., 2020; Spencer et al., 2007). Fourier-transform ion cyclotron resonance mass spectrometry (FT-ICR MS) at 21 T achieves the highest mass resolving power of any current mass analyzer, and can resolve tens of thousands of individual molecular formulae present in DOM, and allows sub-parts-per-million mass accuracy that enables elemental composition assignment and delineates DOM composition and source (Behnke et al., 2021; Hendrickson et al., 2015; Kellerman et al., 2015; Roth et al., 2022). Combining optical parameters with FT-ICR MS analyses allows for in-depth examination of DOM composition and its controlling factors, as well as opening up the potential for developing simple optical proxies for future studies that are tied to arguably the only tool currently available that can handle the complexity of DOM composition (i.e., FT-ICR MS) (Hodgkins et al., 2016; Johnston et al., 2021; Spencer et al., 2014).

In this study, we use 21 T FT-ICR MS and optical analyses to examine the composition of DOM in the Onega River in Western Russia to assess how DOM dynamics in this relatively small northern high-latitude constrained riverine system compares with medium- and large-sized Arctic watersheds; specifically, the Severnaya Dvina and the six largest Arctic rivers. We examine the relationships between CDOM and DOC, as well as DOC and CDOM flux and yield in these systems to assess the accuracy of past model estimates for DOC fluxes from the pan-Arctic watershed. Furthermore, we discuss how estimates incorporating small- and medium-sized Arctic watersheds may impact models of biogeochemical cycling in the Arctic Ocean and the inherent uncertainties in estimating pan-Arctic fluxes based on scaled watershed data. To do this we incorporated data from this study and a literature search to assess DOC yields across the pan-Arctic region, and examined if DOC yields could be predicted from watershed soil C storage (Palmtag et al., 2022) or landscape climate classification (Beck et al., 2018). Additionally, we conducted a scaling exercise by pan-Arctic zones (Figure 1; 1–7) incorporating available DOC yield data to highlight current uncertainty that exists in the Arctic land-ocean DOC flux. Finally, we examine the seasonality of DOC and DOM composition in the Onega River to assess how this system and others like it compare to the well-studied six major Arctic rivers.

2. Methods

2.1. Study Site and Sample Collection

The Onega River is in Northwestern Russia (Figure 1) and has a drainage area of approximately 56,900 km^2, of which approximately 70% is covered by forests and wetlands (Brittain et al., 2009). This permafrost-free watershed is underlain largely by karst limestone bedrock, and groundwater discharge contributes between 30% and 40% of the Onega's annual discharge (Brittain et al., 2009). Water samples were collected between July 2018 and January 2020 ($n = 19$). Sampling occurred approximately every two months between July 2018 and February 2019 and June 2019 and January 2020, and samples were taken multiple times a day between 25 April 2019 and 28 April 2019 to capture high discharge in detail during spring freshet ($n = 9$). Seasons were defined as spring as March through May ($n = 10$), summer as June through August ($n = 4$), fall as September through November ($n = 2$), and winter as December through February ($n = 3$). Samples were taken at 63°49′49.36″N, 38°27′42.12″E during regular discharge and 63°49′41.66″N, 38°28′38.48″E during the spring freshet, about 30 km from the White Sea near the locality of Porog. Water was collected 5–10 m from the river bank and 5–10 cm below the river's surface. Samples were filtered through Whatman GF/F (0.7 μm pore size) filters, which were precombusted at 450°C for 5 hr, the filtered samples were frozen immediately for transport to Florida State University, USA. Discharge data was collected from the ArcticRIMS monitoring station at Porog (station code 70842), which is collected from an ADCP-groundtruthed pressure transducer maintained by Roshydromet (McClelland et al., 2015). ArcticRIMS is a multi-agency initiative to maintain an integrated hydrological monitoring system for the pan-Arctic watershed (rims.unh.edu).

Figure 1. Map showing the pan-Arctic watershed, including the six largest Arctic rivers in light maroon, the Severnaya Dvina (357,000 km^2) in red, and the Onega (56,900 km^2) in blue. The thick black line delineates the boundaries of the pan-Arctic watershed (16.8×106 km^2). The gray numbered regions represent zones between the major watersheds.

2.2. Quantification of Dissolved Organic Carbon and Chromophoric Dissolved Organic Matter

Filtered samples were acidified to pH 2 with 12 M HCl and analyzed for DOC using a Shimadzu high-temperature catalytic oxidation total organic carbon analyzer (TOC-L CPH). DOC concentrations were calculated following protocols established in Johnston et al., 2018; that is, using a six-point standard curve on the average of three to seven injections with a coefficient of variance less than 1% and standard deviation of <0.1 mgL^{-1}.

Absorbance and fluorescence was analyzed on filtered water samples thawed in the dark to room temperature (20°C) and measured using a Horiba Aqualog. DOM absorbance was measured between 230 and 800 nm wavelengths, and fluorescence was measured at excitation wavelengths from 230 to 500 nm and emission wavelengths from 230 to 800 nm. Spectra were normalized and blank corrected using Aqualog software upon measurement, and spectral indices were calculated using the DrEEM MATLAB toolbox (Murphy et al., 2013). Absorbance at 350 nm was converted to Napierian absorbance coefficients (Hu et al., 2002), and used to assess the CDOM content of each sample. The ratio of the absorption coefficients at 250 and 365 nm (a_{250}:a_{365}) was calculated from these values. The a_{250}:a_{365} ratio has been previously related to the aromatic content and molecular size of DOM, with higher values indicative of lower aromaticity and molecular size (Peuravuori & Pihlaja, 1997). Spectral slopes from 275 to 295 nm and from 350 to 400 nm ($S_{275-295}$ and $S_{350-400}$) were calculated and the ratio of these slopes was also calculated as S_R. These values have been previously correlated to DOM molecular weight and aromaticity (Helms et al., 2008; Spencer et al., 2012). SUVA$_{254}$ was normalized to DOC and used as a proxy for aromaticity (Weishaar et al., 2003). Fluorescence index (FI) was calculated as the ratio of the emission intensity at 470 and 520 nm at 370 nm excitation (Cory & McKnight, 2005; McKnight et al., 2001). The humification index (HIX), freshness index (FRESH), and biological index (BIX) were calculated respectively as the area under the emission spectra between 435 and 480 nm divided by the sum of peak areas 300–345 nm and 435–480 nm (Ohno, 2002), the ratio of emission intensity at 380 nm to the maximum emission intensity between 420 and 435 nm at excitation wavelength 310 nm (Parlanti et al., 2000; Wagner et al., 2015), and the ratio of emission intensity at 380 nm divided by 430 nm at excitation wavelength 310 nm (Huguet et al., 2009).

2.3. Solid Phase Extractions and FT-ICR MS

Prior to FT-ICR MS analysis, DOM was isolated via solid phase extraction onto individual PPL cartridges (Agilent Technologies). PPL cartridges were prepared for use by soaking the cartridges in methanol for at least 4 hr, rinsing the soaked cartridges twice with ultrapure water, followed by a methanol rinse (high-performance liquid chromatography (HPLC) grade), followed finally by rinsing twice with ultrapure water acidified to pH 2. Filtered samples were acidified to pH 2 with 12 M HCl before aliquots equivalent to 60 μg C were extracted onto 100 mg PPL cartridges and eluted with HPLC grade methanol into precombusted (450°C, >5 hr) vials to a final concentration of 50 μg OC mL^{-1} (Dittmar et al., 2008). Eluted samples were kept frozen (−20°C) prior to 21 T FT-ICR MS analysis.

Extracted DOM samples were introduced into a custom-built hybrid linear ion trap FT-ICR MS equipped with a 21 T superconducting solenoid magnet using negative electrospray ionization at a flow rate of 500 nL min^{-1} (Hendrickson et al., 2015; Smith et al., 2018) at the National High Magnetic Field Laboratory in Tallahassee, Florida. Mass spectra were phase-corrected (Xian et al., 1998) and internally calibrated with 10–15 highly abundant homologous series that span the entire molecular weight distribution based on the "walking" calibration method (Savory et al., 2011) obtained by co-adding 100 individual transients of 3.1 s mass spectral peaks with a signal magnitude greater than six-times the baseline noise level (6σ). Mass measurement accuracy ≤300 ppb were considered for molecular formula assignment (Blakney et al., 2011). Molecular formulae were assigned to compounds containing $C_{1-100}H_{4-200}O_{1-25}N_{0-2}S_{0-1}$ with PetroOrg©,™ (Corilo, 2015). Compound classes were defined based on elemental ratios and the modified aromaticity index (AI_{mod}) (Koch & Dittmar, 2006). Compound classes included highly unsaturated, low oxygen (HUP, low O/C; $AI_{mod} < 0.5$, H/C < 1.5, O/C < 0.5), highly unsaturated, high oxygen (HUP, high O/C; $AI_{mod} < 0.5$, H/C < 1.5, O/C ≥ 0.5), aliphatic (H/C ≥ 1.5, $N = 0$), condensed aromatic ($AI_{mod} ≥ 0.67$), polyphenolic ($0.67 > AI_{mod} > 0.5$), and peptide like (H/C ≥ 1.5, $N > 0$). Relative abundances of each formula were determined by normalizing each peak magnitude to the sum of all assigned peaks in each sample. Contributions of each compound class to total composition were then calculated as the sum of all the relative abundances of each peak in a given compound class divided by the summed abundances of all assigned formulae. Similar calculations were performed to determine the relative abundance of compounds containing different elemental compositions (e.g., CHO, CHON, CHOS, CHONS). Compounds identified as belonging to the "island of stability" (IOS), a set of 361 presumably highly degraded and stable C-containing formulae found in major oceans (Lechtenfeld et al., 2014), were compared to compounds in Onega River samples and reported as a percent relative abundance. All 21 T FT-ICR MS mass spectra files and elemental compositions are publicly available via the Open Science Framework (https://osf.io/ka5d7/) at: https://doi.org/10.17605/OSF.IO/KA5D7.

2.4. DOC and CDOM Flux and Yield Estimates and Statistical Analysis

DOC and CDOM fluxes and yields were calculated from daily discharge data and either DOC concentration or absorption coefficient data using Fortran Load Estimator (LOADEST) (Runkel et al., 2004). Daily flux calculated using LOADEST was summed to calculate annual fluxes. LOADEST requires a minimum of 12 values across a range of discharge for the model. In this study we used 19 samples encapsulating the range of discharge in the Onega River collected between July 2018 and January 2020. LOADEST uses the method of adjusted likelihood estimation (AMLE) to calculate loads while eliminating collinearity by centering discharge and concentration data, and automatically selects the regression model from nine predefined regression models to fit the data based on the AIC (Akaike Information Criterion). Yield estimates (g m^2 yr^{-1}) were derived by normalization of the loads (Tg yr^{-1}) to the Onega watershed area (km^2). Principle component analysis (PCA) was conducted using the "vegan" package in R (Oksanen et al., 2020). Spearman rank correlations were performed on FT-ICR MS data for variables driving variation on PC1 (DOC, a_{350}, FRESH, and BIX) using the "Hmisc" package in R. Relationships were considered significant if they had a corrected p-value < 0.05.

2.5. Spatial Analysis

Using data from Palmtag et al., 2022 and Beck et al., 2018, we calculated the average C storage (kg C m^2) and area represented by each Koppen-Geiger climate class respectively, within each watershed for the Onega, the Severnaya Dvina, and the largest six Arctic rivers, and the seven remaining zones (1–7; Figure 1) between those
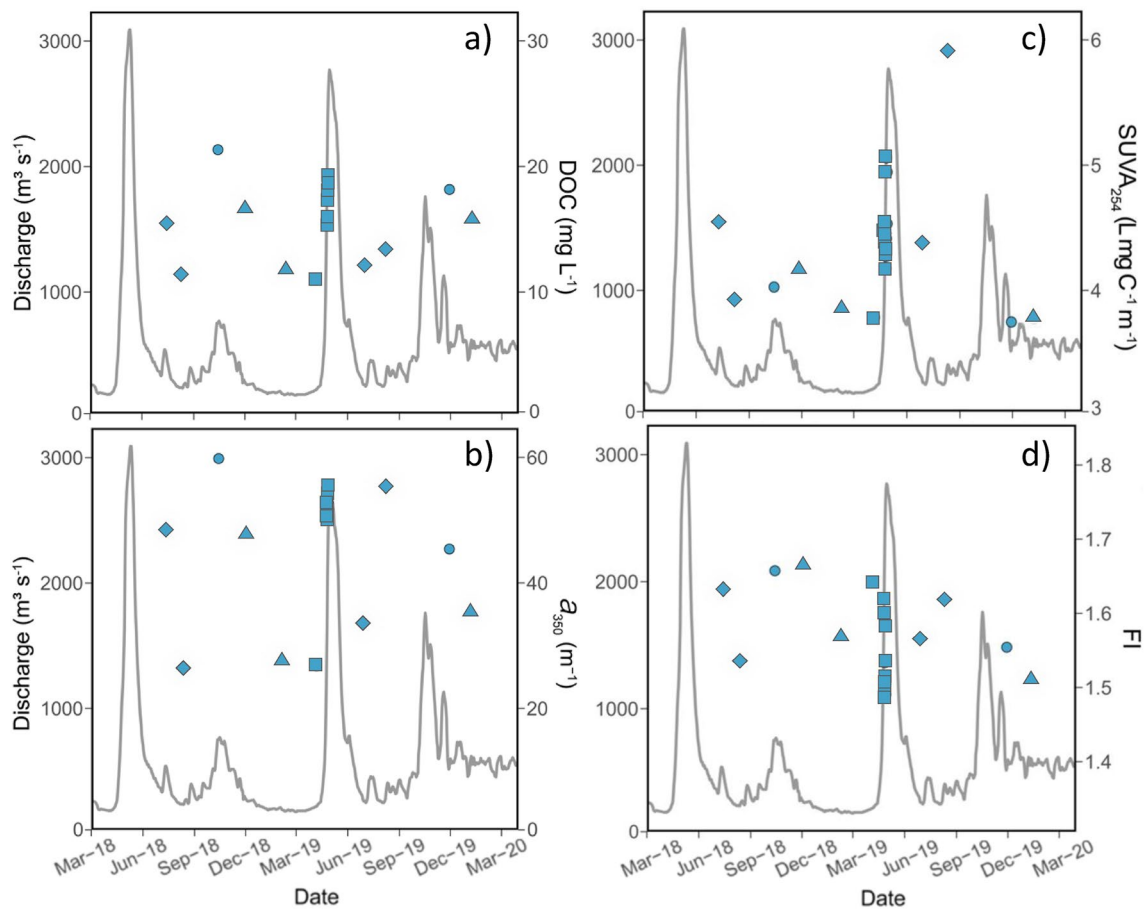
Figure 2. Hydrograph from the Onega River (March 2018 to March 2020) vs. (a) dissolved organic carbon concentration, (b) chromophoric dissolved organic matter absorption coefficient at 350 nm (a350), (c) specific UV absorbance at 254 nm, (d) the fluorescence index. Diamonds represent samples from summer, circles for fall, triangles for winter, and squares for spring.

3. Results

3.1. Onega River Discharge and DOC Concentrations

Discharge in the Onega River ranged from 177 to 3,090 m^3 s^{-1} (Figure 2a) with a mean annual discharge of 1,269 m^3 s^{-1} (Table 1 and Figure 2). Discharge was strongly seasonal, being highest in the spring (mean = 2,035 m^3 s^{-1}), followed by fall (mean = 638 m^3 s^{-1}), and lowest in the summer (mean = 350 m^3 s^{-1}) and winter (mean = 360 m^3 s^{-1}). During the spring freshet, mean discharge was approximately 3–6 times higher than in other seasons. In comparison to 2018–2019, the winter of 2019–2020 was much wetter (Figure S1 in Supporting Information S1) as evidenced by higher discharge and high standard deviation (winter SD = 229 vs. 125 m^3 s^{-1} in summer, Table 1). Concentrations of DOC also varied seasonally, with an annual range of 10.95–21.34 mg L^{-1} and an annual mean concentration of 16.01 mg L^{-1} (Table 1 and Figure 2a). DOC concentrations were highest in the fall and spring (mean = 19.80 and 16.80 mg L^{-1}, respectively) and lowest in the summer and winter (mean = 13.10 and 14.70 mg L^{-1}, respectively). DOC concentrations were higher in seasons with high discharge (i.e., spring and fall) and lowest when discharge was at base flow conditions between February and March 2019.

watersheds to cover the entire Pan-Arctic watershed. DOC yield data for the zones 1–7 (Figure 1) was derived from an extensive search of the literature. To assess whether soil C storage or climate classification related to DOC yield from Arctic rivers, we performed linear regressions to compare the relationship between the average soil C storage, or climate classification percentages in each watershed and DOC yields.

Table 1
Dissolved Organic Carbon (DOC), Discharge, and Optical Data From the Onega River

Variable	Annual			Spring			Summer			Fall			Winter		
	Mean		SD	Mean		SD	Mean		SD	Mean		SD	Mean		SD
Discharge ($m^3 s^{-1}$)	1,269	±	977	2,035	±	707	350	±	125	638	±	160	360	±	229
DOC ($mg C L^{-1}$)	16.01	±	2.87	16.80	±	2.28	13.10	±	1.87	19.80	±	2.24	14.70	±	2.56
a_{350} (m^{-1})	46.1	±	10.6	49.8	±	8.21	40.7	±	13.3	52.6	±	10.2	36.8	±	10.1
SUVA$_{254}$ ($L mg C^{-1} m^{-1}$)	4.35	±	0.53	4.43	±	0.36	4.69	±	0.86	3.89	±	0.20	3.93	±	0.21
FI	1.57	±	0.06	1.55	±	0.06	1.59	±	0.05	1.61	±	0.07	1.58	±	0.08
FRESH	0.50	±	0.03	0.48	±	0.03	0.53	±	0.02	0.50	±	0.03	0.52	±	0.01
BIX	0.51	±	0.03	0.49	±	0.03	0.53	±	0.02	0.51	±	0.03	0.53	±	0.01

3.2. Onega River CDOM Parameters

CDOM absorption coefficient values (a_{350}) in the Onega River ranged from 26.1 to 59.8 m^{-1} (Figure 2b), with an average absorbance of 46.1 m^{-1} ($n = 19$, Table 1). Similar to seasonal variations in DOC, a_{350} was highest in the fall and spring (mean = 52.6 and 49.8 m^{-1}, respectively) and lowest during summer and winter (mean = 40.7 and 36.8 m^{-1}, respectively) (Table 1 and Figure 2b). The highest and lowest a_{350} values were observed during October and August 2018, respectively. This seasonality in a_{350} corresponds positively with discharge apart from one sample collected in August 2019, where high a_{350} was observed concurrently with relatively low DOC and low discharge.

SUVA$_{254}$ in the Onega River ranged from 3.75 to 5.92 $L mg C^{-1} m^{-1}$ with an average value of 4.35 $L mg C^{-1} m^{-1}$ (Figure 2c). The lowest values were observed during the winter and the highest were observed during the spring freshet, with the exception of one sample collected in August 2019 mentioned above. As with SUVA$_{254}$, Onega River average a_{250}:a_{365} values are indicative of highly aromatic DOM (mean = 4.61; Table 1) and also exhibit limited seasonality. $S_{275-295}$ values in the Onega River ranged from 12.60 to 15.09 $\times 10^{-3}$ nm^{-1} with an average value of 13.34 $\times 10^{-3}$ nm^{-1} (Table 1). The lowest $S_{275-295}$ values occurred concurrent with high discharge events during the spring and fall seasons, and the highest values occurred during summer and winter, when discharge was lower. $S_{350-400}$ values ranged from 15.00 to 17.12 $\times 10^{-3}$ nm^{-1} with an average of 16.18 $\times 10^{-3}$ nm^{-1} and S_R ranged from 0.75 to 0.94 with an average of 0.83 (Table 1).

The fluorescence index (FI) has been linked to DOM source, with DOM of microbial origin having an FI of approximately 1.9, and DOM of terrestrial origin having an FI of approximately 1.4 (McKnight et al., 2001). In the Onega River FI ranged from 1.49 to 1.66 (Figure 2d) with an average value of 1.57 (Table 1). FI was lowest in the spring, with the minimum observed value occurring during the spring freshet, and the maximum occurring under-ice in the winter. FRESH, an index which has been observed to increase with greater contribution of recently formed DOM (Fellman et al., 2010; Parlanti et al., 2000), ranged from 0.46 to 0.55 with an average of 0.50 (Table 1). BIX, an indicator of autochthonous DOM (Huguet et al., 2009), ranged from 0.47 to 0.55 with an average of 0.51 (Table 1), with the lowest values occurring during the spring and the highest values occurring in summer.

3.3. Onega River DOM Composition by FT-ICR MS

We observed an average of 15,829 molecular formulae (Table 2), ranging from 14,008 to 18,385 (Figure 3a) in each Onega River sample. The average mass for these formulae ranged from 561.3 to 620.4 Da (Figure 3b) with an average of 595.5 (Table 2). AI$_{mod}$, which suggests the presence of aromatic structures in a given sample of DOM, ranged from 0.35 to 0.39 in the Onega River with a mean of 0.37 and showed some seasonal variation, with values being highest during the spring freshet and fall-to-early-winter samples (Table 2 and Figure 3c). This is highly comparable to AI$_{mod}$ values reported in Amazonian forested streams dominated by terrestrial DOM sources (0.36 ± 0.02 observed in Spencer et al., 2019). Further, this suggests a relative increase in aromatic DOM, which correlates to observed seasonal variations in spectral slope and SUVA$_{254}$ (Table 1 and Figure 3c). Finally, AI$_{mod}$ observed in the Onega River was slightly higher on average than values observed in the Severnaya Dvina (mean = 0.35; Johnston et al., 2018), further underpinning its aromatic nature.

Table 2
Dissolved Organic Matter Composition Data Collected via FT-ICR MS for the Onega River

Variable	Annual Mean		SD	Spring Mean		SD	Summer Mean		SD	Fall Mean		SD	Winter Mean		SD
Number of formulae	15,829	±	1,198	15,539	±	642	16,794	±	1,248	14,752	±	721	16,230	±	2,189
Average mass (Da)	595.5	±	16.6	598.0	±	16.5	585.0	±	15.3	601.0	±	20.8	597.0	±	20.2
AI_{mod}	0.37	±	0.01	0.38	±	0.01	0.37	±	0.01	0.38	±	0.01	0.37	±	0.02
H/C	1.00	±	0.02	1.00	±	0.02	1.01	±	0.01	0.98	±	0.01	1.00	±	0.03
O/C	0.54	±	0.00	0.54	±	0.00	0.54	±	0.00	0.54	±	0.00	0.54	±	0.01
CHO (%)	86.11	±	1.32	86.47	±	1.13	85.04	±	0.92	87.09	±	0.46	85.66	±	2.05
CHON (%)	9.41	±	0.47	9.16	±	0.40	10.02	±	0.63	8.94	±	0.04	9.55	±	0.62
CHONS (%)	0.54	±	0.10	0.53	±	0.04	0.53	±	0.07	0.52	±	0.00	0.61	±	0.24
CHOS (%)	3.97	±	0.76	3.84	±	0.74	4.41	±	0.51	3.45	±	0.42	4.18	±	1.20
Condensed aromatics (% RA)	5.06	±	0.75	5.36	±	0.65	4.51	±	0.57	5.56	±	0.25	4.49	±	0.96
Polyphenolics (% RA)	17.91	±	1.38	18.26	±	1.26	17.18	±	1.06	18.78	±	1.06	17.15	±	2.11
Aliphatics (% RA)	3.06	±	0.40	3.15	±	0.32	3.20	±	0.26	2.66	±	0.36	2.82	±	0.70
Peptide-like compounds (% RA)	0.04	±	0.04	0.04	±	0.03	0.08	±	0.04	0.02	±	0.01	0.05	±	0.04
HUP, high O/C (% RA)	48.94	±	1.57	48.13	±	1.44	49.79	±	1.46	48.78	±	0.71	50.62	±	0.69
HUP, low O/C (% RA)	24.04	±	1.00	24.11	±	0.81	24.38	±	0.70	23.19	±	0.24	23.96	±	2.09
IOS (% RA)	17.31	±	2.32	16.66	±	2.02	18.73	±	1.92	16.24	±	1.95	18.31	±	3.75

DOM elemental composition exhibited little seasonal variation. Percent relative abundance (% RA) of CHO ranged from 83.53% to 87.91% RA, with a mean of 86.11% (Table 2). CHON ranged from 8.64% to 10.94% RA (Figure 3d and Table 2). CHONS ranged from 0.40% to 0.87% RA with a mean of 0.54% RA, and CHOS, ranged from 2.96% to 5.70% RA with a mean of 3.97% RA, respectively (Table 2). Condensed aromatic and polyphenolics, compounds derived from terrestrial or allochthonous sources (Kellerman et al., 2015; Koch & Dittmar, 2006), in the Onega River ranged from 3.79% to 6.15% RA with a mean of 5.06% RA, and from 15.73% to 19.62% RA with a mean of 17.91% RA, respectively (Figure 3e and Table 2). The % RA of these aromatic compounds combined peaked during the spring freshet, and the contribution of allochthonous compounds to DOM composition was also increased in the fall relative to summer and winter (Figure 3e and Table 2). The standard deviation for both condensed aromatics and polyphenolics was highest during the winter (0.96 and 2.11, respectively, Table 2), suggesting the greatest variability within these compound classes during the winter. Aliphatic and peptide-like compounds contributed between 2.03% and 3.69% RA, and 0.002% and 0.14% RA respectively, with respective averages of 3.06% and 0.04% RA (Figure 3f andTable 2). These compounds are typically associated with highly biolabile DOM (Spencer et al., 2015; Textor et al., 2019), possibly of microbial or autochthonous origin (Kellerman et al., 2018; Spencer et al., 2015; Textor et al., 2019), and their relatively low contributions and little seasonal variability suggest that DOM exported by the Onega is primarily terrestrial in origin. The majority of the assigned formulae belonged to the highly unsaturated and phenolic (HUP) class, with low O/C HUPs ranging from 21.66% to 25.74% RA with a mean of 24.04% RA, and high O/C HUPs ranging from 45.32% to 51.57% RA with a mean of 48.94% RA (Table 2). This dominance of HUP-assigned formula is similar to past studies examining riverine DOM globally (Behnke et al., 2021; Kellerman et al., 2018; Kurek et al., 2021; Spencer et al., 2019).

DOM composition as determined by FT-ICR MS showed minimal seasonal variability in compound classes in the Onega River (Figure 4a). In comparison to the six largest Arctic rivers the overall annual composition in the Onega River appears to be more terrestrial in origin, with condensed aromatics and polyphenolics contributing relatively more (Figure 4b). Compounds belonging to the IOS ranged from 13.98% to 20.82% RA (mean = 17.31% RA; Table 2) and exhibited lower relative contributions in the spring and the fall. This range is close to the lower end of that observed in the six largest Arctic rivers, where IOS values were lowest during freshet and highest in winter (~30% RA), and the average IOS value in the Onega (17.31% RA; Table 2) is even lower than that observed in the six largest Arctic rivers across spring freshet at around 23%–26% RA (Behnke et al., 2021), clearly showing the dominance of terrestrial sourced highly aromatic DOM in this system.
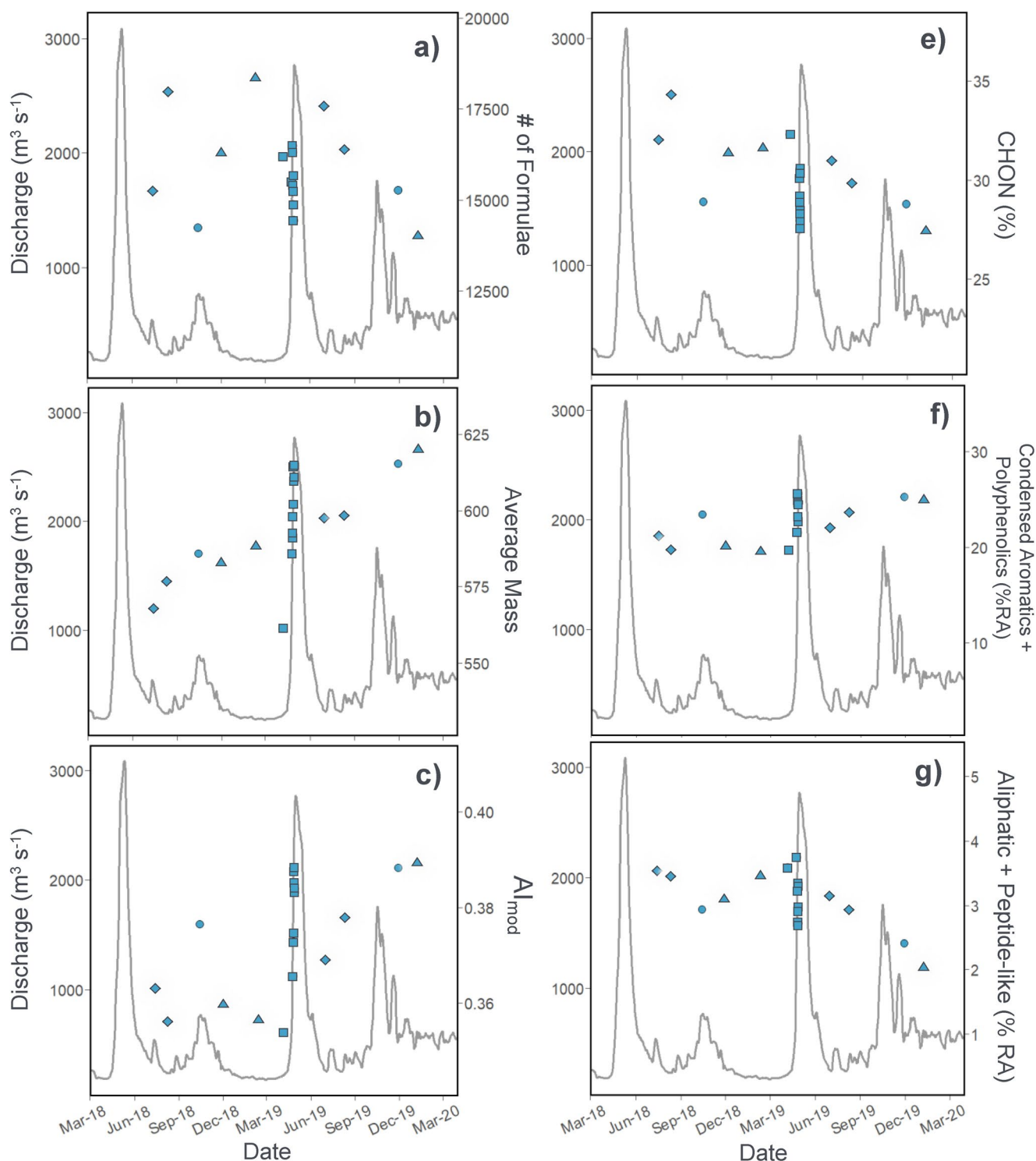
Figure 3. Hydrograph from the Onega River (March 2018 to March 2020) vs. (a) number of formulae, (b) average mass, (c) modified aromaticity index (AImod), (d) percent CHON, (e) the percent relative abundance of condensed aromatics and polyphenolics, and (f) the percent relative abundance of aliphatics and peptide-like compounds. Diamonds represent samples from summer, circles for fall, triangles for winter, and squares for spring.
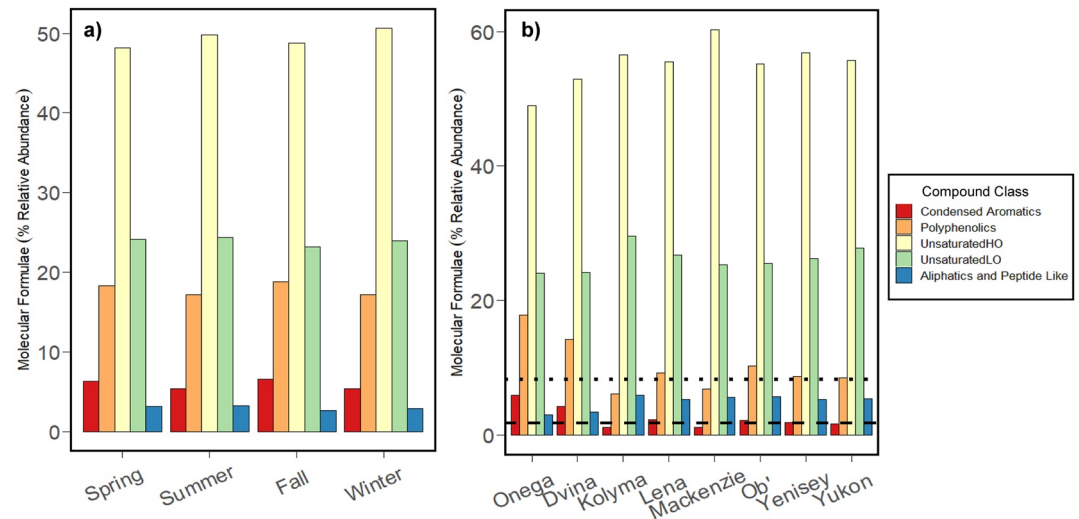
Figure 4. Dissolved organic carbon composition represented as percent relative abundance by compound class comparing (a) season in the Onega River and (b) river, including the six largest Arctic rivers, the Severnaya Dvina, and the Onega. From left to right, the bars in each panel represent condensed aromatics, polyphenolics, highly unsaturated and phenolic (high O/C), highly unsaturated and phenolic (low O/C), and both aliphatics and peptide-like compounds. The dashed line in panel b represents the average percent relative abundance for condensed aromatics in the six largest Arctic rivers, and the dotted line represents the average percent relative abundance for polyphenolics in the six largest Arctic rivers.

3.4. Investigating Controls on Onega River DOM Composition

A PCA on CDOM and FT-ICR MS parameters was conducted to investigate patterns in seasonality and discharge for each sample (Figure 5). PC1 explained 54.1% of the variance and was driven negatively by DOC concentration, a_{350}, and the %RA of condensed aromatics and polyphenolics, and positively by CHON, FRESH and BIX indices (Figure 5; Table S1 in Supporting Information S1). PC2 explained 18.9% of the variance and was driven
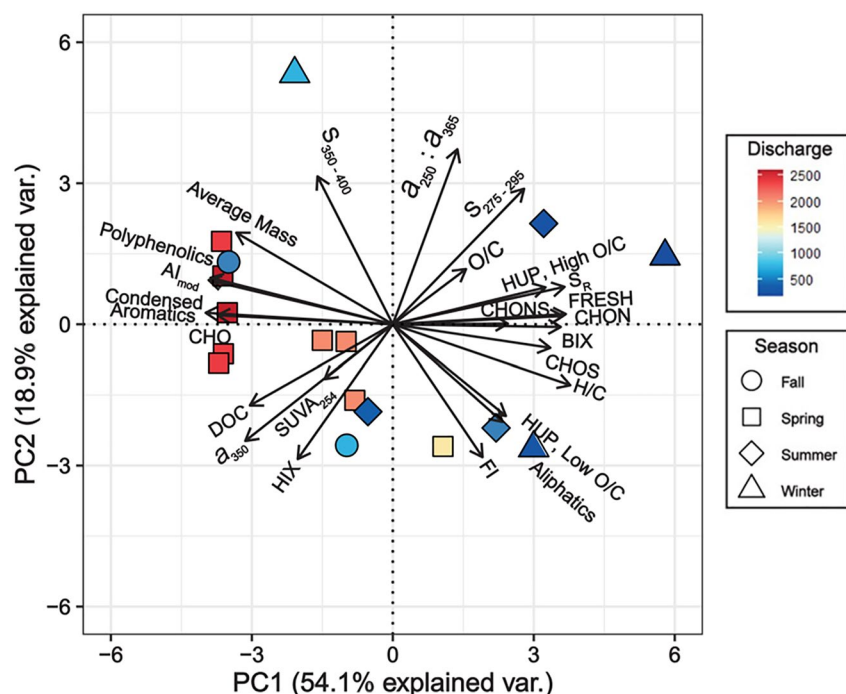

Figure 5. Principal components analysis of optical and compositional parameters in Onega River samples. Discharge (m3 s^{-1}) is depicted by color and season is depicted by shape. All parameters are as defined in the text.
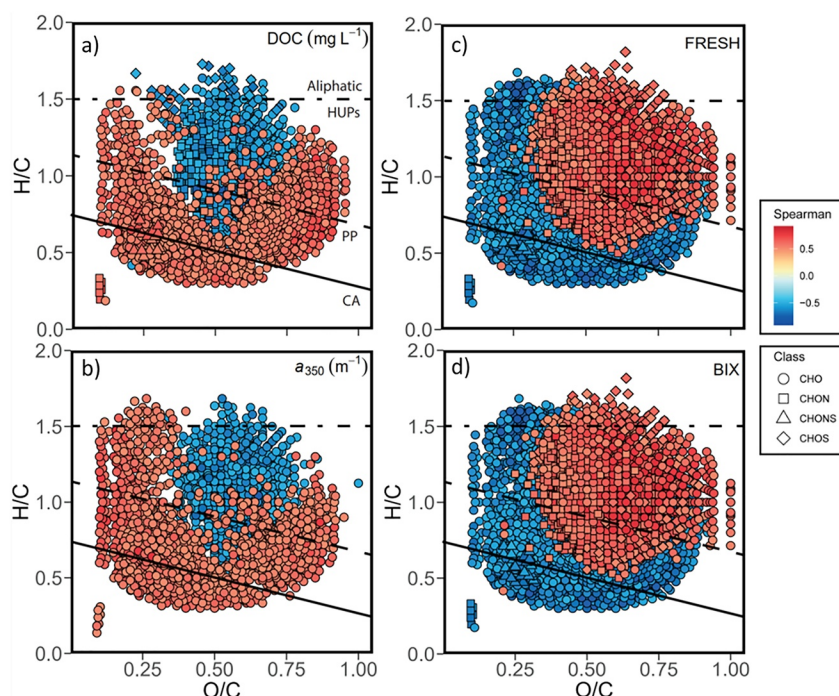
Figure 6. Significant Spearman correlations ($P < 0.05$) between relative intensities of compounds identified by FT-ICR MS and the four strongest drivers of PC1: (a) dissolved organic carbon concentration, (b) chromophoric dissolved organic matter (a350), (c) freshness index index, and (d) biological index index. The heteroatom class of individual compounds is depicted by shape, and Spearman correlations are depicted with a color gradient from −1.0 to 1.0. Compound class delineations are labeled in panel (a) and from top to bottom, depict Aliphatic, high unsaturated and phenolic, PP (polyphenolic), and CA (condensed aromatics) compound classes.

positively by $a_{250}:a_{365}$ and spectral slope parameters and negatively by FI and HIX (Figure 5; Table S1 in Supporting Information S1). It is apparent that fall and spring samples group together into the left quadrants of the PCA visualization and this seasonal distribution of loadings supports our observation that fall discharge events may be chemically similar to the spring freshet. We performed Spearman's rank correlations between the intensities of molecular formulae identified by FT-ICR MS and the optical parameters identified as having the strongest effect on PC1 (Figure 6) in order to validate optical measurements using FT-ICR MS data in the Onega River. Each of these van Krevelen's diagrams (Figure 6) are further visualized by heteroatom class in Figures S2–S5 in Supporting Information S1.

3.5. Onega River DOC and CDOM Fluxes and Yields

An estimated 0.28 Tg of DOC is exported annually from the Onega River (Table S2 in Supporting Information S1), a smaller flux than observed from the nearby Severnaya Dvina (1.19 Tg yr^{-1}) and the six largest Arctic rivers (18.11 Tg yr^{-1}) (Holmes et al., 2012; Johnston et al., 2018). This is unsurprising as the Onega is much smaller in size and in discharge than these other Arctic rivers; being about six times smaller than the Severnaya Dvina Basin and an order of magnitude smaller than the Kolyma, the smallest of the largest six Arctic rivers. However, when normalized to watershed area, the Onega DOC yield was estimated at an average of 4.85 g m^2 yr^{-1}, a higher yield than observed in the largest six Arctic rivers (0.82–2.34 g m^2 yr^{-1}) and the Severnaya Dvina (3.33 g m^2 yr^{-1}) (Holmes et al., 2012; Johnston et al., 2018). The high DOC yield from the Onega River is comparable to yield values reported in other smaller northern high-latitude constrained terrestrially dominated systems in Alaska (Johnston et al., 2021) and with values observed in northern boreal peatlands (Evans et al., 2016).

The Onega exports 0.66 m^2 yr^{-1} of CDOM annually, estimated using a_{350} measurements (Table S3 in Supporting Information S1). Annual CDOM yield is estimated at 9.94 yr^{-1}. This is similar to CDOM yields observed
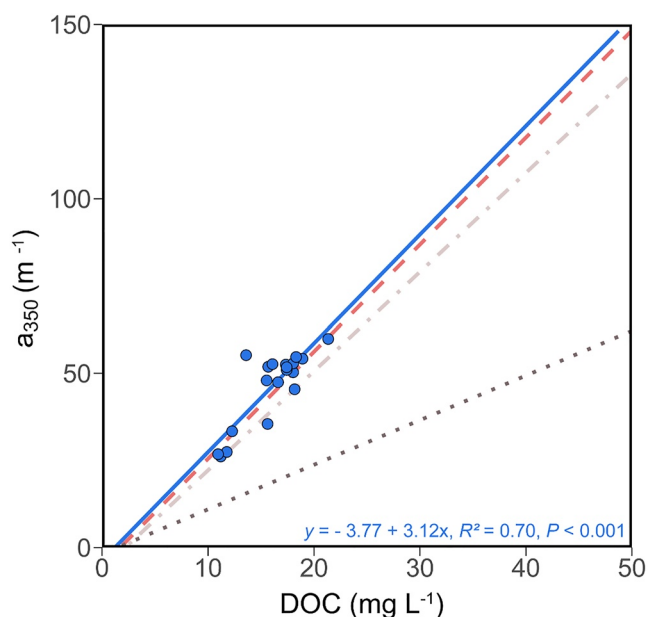
Figure 7. Relationship between dissolved organic carbon and chromophoric dissolved organic matter (a350) for the Onega River (blue solid line, blue circles), the Severnaya Dvina (red dashed line), the six largest Arctic rivers (the light maroon dot/dash line) and the Rio Grande (gray dotted line).

from the Atchafalaya ($9.20 \ yr^{-1}$) and Edisto ($12.63 \ yr^{-1}$) Rivers in the United States, both of which drain extensive organic-rich wetlands (Spencer et al., 2013). There was a strong relationship between CDOM and DOC in the Onega River (Figure 7).

3.6. Spatial Analysis and Basin Characterization

DOC yields from this study or estimated from literature data, percent area of each Koppen-Geiger climate class, and soil C storage for each of the six major Arctic rivers, the Severnaya Dvina, the Onega, and the seven remaining pan-Arctic zones (Figure 1) are presented in Table 3. Linear regressions performed between either soil C storage (Figure S6 in Supporting Information S1) or climate class percentages and DOC yields in Arctic rivers and zones had coefficients of determination for C storage and DOC yield of 0.03, and for Koppen-Geiger classes and DOC yield ranged from 0.0065 to 0.28. Therefore, there was no apparent relationship between either soil C storage or climate class with DOC yield.

4. Discussion

4.1. Comparisons Between the Onega River and Other Arctic Fluvial Systems

The observed DOC concentrations in the Onega River are higher than those observed in the six largest Arctic rivers (Holmes et al., 2012; Mann et al., 2016), as well as other medium sized Arctic rivers like the Severnaya Dvina (Johnston et al., 2018) and the Mezen Rivers (Lobbes et al., 2000), both of which also drain into the White Sea. The elevated DOC concentration in the Onega River is particularly apparent outside of the freshet when DOC concentration is comparatively lower in the major Arctic rivers (Behnke et al., 2021; Holmes et al., 2012; Mann et al., 2016). For example,

DOC concentration in the Onega River in the winter was on average $14.70 \ mg \ L^{-1}$ while the winter DOC concentration for the Ob' (which has the most elevated winter DOC concentration of the six largest Arctic rivers) ranges from ~7.6 to $9.2 \ mg \ L^{-1}$ (Behnke et al., 2021; Mann et al., 2016). Similar to the six largest Arctic rivers, discharge is highest during the spring freshet, but unlike those watersheds, DOC concentrations are also high during the fall. Previous measurements of seasonal DOC concentrations in Arctic rivers have typically included the samples which we have defined as "fall" as part of either summer or winter and report lower averages in DOC concentration (Behnke et al., 2021; Holmes et al., 2012; Mann et al., 2016). This fall peak in DOC concentration corresponds to high discharge events during the fall, which have been observed in other small-to-medium sized Arctic rivers (Dankers & Middelkoop, 2007; Johnston et al., 2018; Lobbes et al., 2000), but are not readily apparent in the six largest Arctic rivers (Holmes et al., 2012; Raymond et al., 2007; Spencer et al., 2008).

The average a_{350} value in the Onega River is higher than that observed in other Arctic rivers (Johnston et al., 2018, 2021; Mann et al., 2016; Spencer et al., 2008), and the highest value observed during the fall in the Onega ($52.6 \ m^{-1}$) is similar to the highest value observed in the Severnaya Dvina ($56.40 \ m^{-1}$) and a blackwater tributary of the Yukon River ($58.52 \ m^{-1}$) (Johnston et al., 2018; Spencer et al., 2008). Samples taken under-ice and during low flow conditions during summer were also higher than a_{350} values measured in the six major Arctic rivers during the same time of year (Johnston et al., 2018; Mann et al., 2016; Spencer et al., 2008). For example, Mann et al., 2016 observed under-ice a_{350} values from the Ob' and the Yenisey to be as low as 13.1 and $7.1 \ m^{-1}$, respectively, while we observed our lowest under-ice a_{350} to be $27.4 \ m^{-1}$. These values are similar to the relatively high under-ice values observed in the Severnaya Dvina (Johnston et al., 2018).

The average $SUVA_{254}$ value ($4.35 \ L \ mg \ C^{-1} \ m^{-1}$, Table 1), which suggests that DOM exported by the Onega River is predominantly aromatic in nature year-round, is higher than that observed in the six major Arctic watersheds

Table 3

Average Dissolved Organic Carbon (DOC) Yield, Basin Climate Classification, and Average Soil (0–300 cm) C Storage for the Seven Regions (Figure 1), Six Largest Arctic River Basins, the Onega and the Severnaya Dvina

Region	Basin area (km²)	DOC yield (g m⁻² yr⁻¹) Min	Max	Average yield	n	Yield source	Min DOC flux (Tg yr⁻¹)	Max DOC flux (Tg yr⁻¹)	Average DOC flux (Tg yr⁻¹)	Bwk area (%)	Bsk area (%)	Ds area (%)	Dw area (%)	Df area (%)	ET area (%)	C storage (kg C m²)[12]
1	905,829	1.18	6.73	3.56	10	1, 2*, 3	1.07	6.10	3.22	0.0	0.0	0.0	0.0	95.0	4.2	44.9
2	638,838	0.19	4.32	1.29	33	2*, 4	0.12	2.76	0.83	0.0	0.0	0.0	0.0	80.5	18.8	54.5
3	1,194,705	0.9	1.63	1.37	5	1, 2*, 5	1.08	1.95	1.64	0.0	0.0	0.0	0.8	59.6	39.1	47.3
4	891,389	0.03	1.31	0.71	9	1, 2*, 5	0.03	1.17	0.63	0.0	0.0	9.2	19.3	34.1	37.0	46.1
5	447,785	2.1	2.1	2.1	1	2*	0.94	0.94	0.94	0.0	0.0	20.5	0.0	20.7	57.7	53.8
6	338,381	0.4	2.14	1.55	7	6, 7, 8	0.14	0.72	0.52	0.0	0.0	25.0	0.0	36.0	37.9	53.6
7	842,225	0.33	1.91	0.89	12	8	0.28	1.61	0.75	0.0	0.0	21.7	4.0	45.5	28.2	55.0
Kolyma	650,000	–	–	1.56	1	9	–	–	0.82	0.0	0.0	26.2	8.0	53.7	12.1	51.2
Lena	2,460,000	–	–	2.34	1	9	–	–	5.68	0.0	0.0	3.6	29.6	64.0	2.7	40.8
Mackenzie	1,780,000	–	–	0.82	1	9	–	–	1.38	0.0	0.0	10.5	0.0	81.1	8.4	39.4
Ob'	2,990,000	–	–	1.40	1	9	–	–	4.12	0.3	21.8	0.0	0.5	76.3	1.2	43.1
Yenisey	2,540,000	–	–	1.90	1	9	–	–	4.65	0.0	3.1	0.0	31.1	61.6	4.2	39.8
Yukon	830,000	–	–	1.77	1	9	–	–	1.47	0.0	0.7	23.5	1.9	60.3	13.6	32.4
Severnaya Dvina	357,000	–	–	3.33	1	10	–	–	1.19	0.0	0.0	0.0	0.0	100.0	0.0	53.5
Onega	56,900	–	–	4.85	1	This study	–	–	0.28	0.0	0.0	0.0	0.0	100.0	0.0	49.3

Note. Yield sources: 1. Dittmar and Kattner (2003), 2. V. Gordeev et al. (1996)*, 3. V. V. Gordeev and Kravchishina (2009), 4. Frey and Smith (2005), 5. Lobbes et al. (2000), 6. Speetjens et al. (2022), 7. McClelland et al. (2014), 8. Li Yung Lung et al. (2018), 9. Holmes et al. (2012), 10. Johnston et al. (2018) 11. Beck et al. (2018) 12. Palmtag et al. (2022) *V. Gordeev et al. (1996) contains values for TOC only, the sum of both DOC and particulate organic C. We have included this because V. Gordeev et al. (1996) estimates that DOC makes up 86%–91% of TOC in most Arctic rivers.

Koppen-Geiger Classifications: BWk represents cold arid desert. BSk represents cold arid steppe. Ds area represents the total area of all cold, dry summer climates and is the sum of the subclasses Dsb (warm summer), Dsc (cold summer) and Dsd (very cold winter). Dw area represents the total area of cold, dry winter climates and is the sum of the subclasses Dwb (warm summer), Dwc (cold summer) and Dwd (very cold summer). Df area represents the total area of cold climates with no dry season, and is the sum of the subclasses Dfa (hot-summer), Dfb (warm summer), Dfc (cold summer), and Dfc (very cold winter). ET represents the total area of tundra.

and higher than that reported for the Severnaya Dvina (mean = 3.97 L mg C⁻¹ m⁻¹ in the Dvina), which has been previously described as having the highest SUVA$_{254}$ value in examined Arctic rivers to-date (Johnston et al., 2018; Mann et al., 2016; Spencer et al., 2008; Stedmon et al., 2011). With an average FI of 1.57, the Onega River is similar to other blackwater systems (∼1.5) including the Severnaya Dvina (mean = 1.59) (Johnston et al., 2018; McKnight et al., 2001; Spencer et al., 2010). Average FRESH index values are similar to those found in thawed permafrost and in other small high-latitude rivers in Alaska (Mutschlecner et al., 2018; Selvam et al., 2017). BIX values observed in the Onega are lower than those described for the Yukon River, which has BIX values consistent with high inputs of terrestrial DOM (Lin et al., 2021), signifying even greater relative inputs in the Onega. Taken together, all the CDOM parameters highlight that DOM in the Onega River has a highly terrestrial contribution.

DOM composition in the Onega River is dominated by terrestrial sources of DOM throughout the year. This is supported by both optical and FT-ICR MS parameters, including high average SUVA$_{254}$ values and high AI$_{mod}$ values (Figures 2c and 3c). DOM dynamics also exhibited seasonal variation, with DOC concentration, absorbance parameters, and AI$_{mod}$ showing consistent patterns with elevated discharge in spring and fall, compared to lower discharge during summer and winter. These variations indicate a flush of aromatic, high molecular weight DOM with high discharge events in the spring and fall, consistent with compositional changes observed with

storm and snowmelt events in other forested watersheds (Inamdar et al., 2006; Raymond & Saiers, 2010; Wagner et al., 2019). Condensed aromatics and polyphenolics increased in relative abundance during these periods as well, indicating a greater relative proportion of allochthonous DOM (Table 2). These compound classes occur in higher proportions in both the Onega and the Severnaya Dvina compared to the six largest Arctic rivers, further supporting the need to include smaller watersheds in pan-Arctic studies (Figure 4b). However, individual compound classes showed little seasonal variation in comparison to the major Arctic rivers (Figure 4), and are generally relatively stable across the year, regardless of DOC concentration or discharge characteristics. In contrast, there are marked seasonal differences in the relative abundances of IOS and compound classes in the six largest Arctic rivers (Behnke et al., 2021). Periods of elevated discharge in the fall prior to freezing occurred in both years of the sampling period (Figure S1 in Supporting Information S1), concurrent with relatively high DOC concentrations, a_{350} values, and SUVA$_{254}$ values. DOM compositional changes with spring discharge events have been well documented in the spring in both large and small northern high-latitude rivers (Amon et al., 2012; Behnke et al., 2021; Holmes et al., 2012; Kaiser et al., 2017). In the Onega, DOM during the fall had the highest average mass, CHO %, and condensed aromatics % RA and the lowest contribution of aliphatic and peptide-like compounds, observed across the year (Table 2). This suggests that fall DOM is more stable and aromatic in nature, and relatively more terrigenous than in other seasons, similar to findings in the Dvina River (Johnston et al., 2018).

4.2. Controls on DOM Dynamics in the Onega River

The observed potential phenomenon of a fall terrestrial flush appears to be mostly absent from the largest six Arctic rivers although we recognize the limitations in datasets that may not have captured this due to sampling temporal resolution. However, elevated discharge events prior to onset of freezing appear to be a normal feature in the annual hydroperiod in similar rivers, with increased discharge events in the fall being observed in the Severnaya Dvina and Mezen Rivers in Western Russia and other high-latitude Arctic rivers like the Tana, the Alta, and the Pechora (Dankers & Middelkoop, 2007; Johnston et al., 2018). We propose that as temperatures drop and precipitation events occur more frequently in the fall (Wang et al., 2021; Yu & Zhong, 2021), an "autumn squeeze" may occur as peatlands freeze and thaw, essentially "wringing out" C rich soils into the Onega and other northern high-latitude peatland-draining rivers. Another potential explanation for this peak in DOC concentration during the fall is that the small size of the Onega essentially "amplifies" the signal of increased precipitation in the fall relative to the summer and subsequent increased discharge. However, it is important to consider the limited number of observations from the Onega River in the fall ($n = 2$). These events may represent a significant biogeochemical phenomenon in these systems similar in magnitude to the spring freshet, but further research is necessary to confirm these findings and begin to understand how they may change into the future as the Arctic hydrologic cycle changes and intensifies (Rawlins et al., 2010).

Interestingly, DOM in the Onega River remains chemically similar and largely terrestrially dominated even during winter base flow conditions, when groundwater flow is the dominant source of runoff in northern high-latitude watersheds (Kaiser et al., 2017; Prowse et al., 2006; Striegl et al., 2005). Higher average SUVA$_{254}$ values annually and in winter suggest DOC-rich groundwater in the Basin. These values are similar to observations from blackwater systems like the Tolovana and Black Rivers in Alaska (Johnston et al., 2021; Spencer et al., 2008) and the Chowan, Kissimmee, and Suwannee Rivers in the Southern United States (Kurek et al., 2020; Leech et al., 2016). SUVA$_{254}$ has been linked to peatland cover extent in a variety of locations, including in Great Britain (Williamson et al., 2021), the Congo (Lambert et al., 2016), and the Arctic (Olefeldt et al., 2013; O'Donnell et al., 2016). DOC concentration also remained high during the winter, in contrast to the largest Arctic rivers where baseflow is characterized by lower DOC concentrations and more allochthonous contributions of DOM (Behnke et al., 2021; Mann et al., 2016). Finally, the FT-ICR MS data clearly highlights a muted seasonality and greater relative contribution from polyphenolics and condensed aromatics in the Onega across the year in comparison to that observed in the six major Arctic Rivers (Figure 4). These characteristics suggest a sustained DOM source throughout the year, potentially from peatlands and peat-influenced groundwater. These differences in seasonal and annual DOM composition further highlight the issues with scaling estimates or inferring DOM seasonal dynamics from the largest Arctic rivers to smaller watersheds constrained to northern high-latitudes.

4.3. Relating DOM Characteristics and Optical Measurements

It is apparent that a_{350} and DOC concentration exhibited similar patterns in variation that corresponded with discharge (Figures 2a and 2b), and a strong correlation was found between a_{350} and DOC concentration (Figure 7, $r^2 = 0.70$, $p < 0.01$) in agreement with correlations observed from other terrestrially dominated rivers (Johnston et al., 2018; Mann et al., 2016; Spencer et al., 2013). With respect to the Onega a slightly steeper slope in the linear regression between a_{350} and DOC is apparent (blue solid line; Figure 7) compared to the six largest Arctic rivers (light maroon dashed-dot line; Figure 6), suggesting that the Onega River transports more CDOM per unit DOC than rivers draining larger catchments and is similar to results found by Johnston et al., 2018 focused on the Severnaya Dvina (red dashed line; Figure 7). If we compare this relationship in the Onega to that reported for the Rio Grande (gray dotted line; Figure 7), a large river dominated by autochthonous DOM, we observe a significant increase in exported CDOM per unit DOC, likely from the larger proportion of allochthonous inputs in the Onega and other Arctic rivers dominated by more aromatic DOM sourced from the terrestrial landscape (Figure 4). This supports the findings of Johnston et al., 2018, showing that if the relationship between CDOM and DOC from the six largest Arctic rivers were to be applied to smaller watersheds such as the Onega, DOC concentrations would be systematically underestimated. For example, using the formula from the linear regression of the six largest Arctic rivers (Figure 7), with an input absorbance of 46.14 m^{-1} (the annual average value in the Onega), DOC in the Onega would be estimated at approximately 16.0 mg L^{-1} and estimated at approximately 18.5 mg L^{-1} in the major six Arctic rivers.

The PCA conducted on the DOM compositional and optical data show clear correlations between optical measurements and data generated through FT-ICR MS. The FRESH and BIX indices, for example, almost exactly overlap the loadings for CHONS and CHON respectively, which indicates a new potential use for these indices as proxies for heteroatom classes that deserves further exploration in future studies. BIX, and specifically the fluorophore it is related to, has been previously seen as relating to biological activity in coastal waters (Huguet et al., 2009; Parlanti et al., 2000), and both the PCA and Spearman correlations suggests that both BIX and FRESH may be also be related to the relative abundance of HUPs and aliphatic compounds (Figures 6 and 7). This supports previous studies centered on samples from the marine environment and Arctic lakes where BIX has been correlated with microbial DOM production (Huguet et al., 2009; Kellerman et al., 2018). The relationship between FI and the relative abundance of aliphatics and low O/C ratio HUPs provides further evidence of the link between FI and DOM composition and source (McKnight et al., 2001). The similar relationship between SUVA$_{254}$ and FT-ICR MS parameters linked to aromaticity (e.g., AI$_{mod}$, condensed aromatics, polyphenolics) highlighted in the PCA (Figure 5) also adds weight to past studies that have shown the ability to link these analyses (Kellerman et al., 2018). Finally, as noted above the strong relationship between DOC and a_{350} in the Onega River (Figure 7) allows for future studies to derive improved DOC flux estimates from in situ CDOM sensors, which is particularly important for capturing the highly dynamic events in the spring and the fall.

Onega River DOC concentrations were significantly correlated (absolute-value Spearman's rank correlation coefficient, $\rho_s \geq 0.49$; $p < 0.05$) to 2,778 molecular formulae (13%) with a clear separation in van Krevelen space of formula with similar ρ_s values and signs into two groups (Figure 6a). CDOM (a_{350}) was similarly significantly correlated with 2,504 molecular formulae (11%) and exhibited a similar pattern in van Krevelen space to DOC (Figure 6b). FRESH and BIX indices were significantly correlated to 7,859 and 7,962 molecular formulae respectively (37% and 38%) and with similar patterns of separation in van Krevelen space inverse to those of DOC and a_{350}. Ultimately, the similarity in molecular assemblages in van Krevelen space between DOC and a_{350}, as well as DOM optical compositional parameters such as FRESH and BIX shows the ability to utilize simple optical proxies to assess the changing DOM composition driven by hydrology in the Onega River system. Thus future studies can not only robustly examine DOC concentration in aquatic systems via CDOM (Figure 7), but may also utilize in situ sensors and simple optical measurements to investigate DOM composition.

4.4. Characterizing Uncertainty in Estimating DOC Flux to the Arctic Ocean

Estimates of riverine DOC export into the Arctic Ocean have been previously scaled up to the remaining ~33% of pan-Arctic watershed area (Figure 1; 16.8×10^6 km^2) using data collected from the six major Arctic rivers, despite heterogeneity across smaller watersheds in regards to latitude, permafrost extent, and landcover type (Holmes et al., 2012; Johnston et al., 2018). This area is dominated by northern high-latitude constrained rivers (Figure 1) and encompasses 5.5×10^6 km^2. The DOC flux from the 11.3×10^6 km^2 watershed area drained by the

six major Arctic Rivers has been estimated at 18.1 Tg yr^{-1} which scales to a pan-arctic DOC flux of 27.3 Tg yr^{-1} (Holmes et al., 2012; Johnston et al., 2018). If the estimated DOC flux from the Severnaya Dvina (1.19 Tg yr^{-1}; Johnston et al., 2018) is also added to the flux from the six major rivers, a DOC flux of 19.3 Tg yr^{-1} is accounted for. If the DOC yield from the Severnaya Dvina is taken as representative of the remaining unmeasured portion of the pan-Arctic watershed this has been estimated to result in a DOC flux of 36.9 Tg yr^{-1} (Johnston et al., 2018). Here, taking the even higher DOC yield found in the Onega River (4.85 g m^2 yr^{-1}; Table 3) as representative of the remaining unmeasured portion of the pan-Arctic watershed this results in a potentially even greater pan-Arctic DOC flux of 45.08 Tg yr^{-1}. This difference in DOC flux between even past estimates scaling from the Severnaya Dvina is equivalent to over three times the annual load from the Mississippi River (Spencer et al., 2013), or, more relevantly, roughly equivalent to finding a flux from watersheds the size of the Lena and the Yukon combined unaccounted for in the Arctic land-ocean flux (Holmes et al., 2012).

To further highlight the uncertainties inherent to upscaling DOC yields, we used available literature values of DOC yield (Table 3) for each of the unnamed regions between the major basins and applied the same upscaling calculations for each of the seven regions. Using the average DOC yield in each of the seven regions and scaling up by region, we estimated a pan-Arctic DOC flux of 28.11 Tg yr^{-1} (Table 3), slightly higher than that estimated in Holmes et al., 2012 simply from scaling from the major six Arctic rivers (27.3 Tg yr^{-1}). However, the range of available DOC yield data for each of the seven regions is quite broad in all cases, and thus minimum and maximum bounds can be placed on these regions. Taking the known DOC fluxes from the major six Arctic rivers and the Severnaya Dvina and Onega (19.58 Tg yr^{-1}; Table 3), and adding the potential minimum and maximum DOC fluxes from the seven regions results in a range of total DOC flux from 23.24 to 34.83 Tg yr^{-1} (Table 3).

A large source of this uncertainty comes from significant temporal and spatial gaps in sampling efforts. Logistical challenges in Arctic environments generally restrict sampling to summer months, thus many sampling efforts miss the spring thaw period where high DOC concentrations concurrent with high discharge result in large amounts of DOC transported in a short burst of time. One study estimated that as much as 30% of the annual DOC export from the Kuparuk River in Alaska occurs in the spring and fall, and suggests that these temporal biases may cause systematic underestimates of Arctic DOC fluxes (Shogren et al., 2020). Similarly, Arctic rivers and streams are often remote and challenging areas for field work, and thus sampling efforts have largely been constrained either to the six largest rivers or to areas with existing infrastructure (like those near established research stations). These issues combine to create large uncertainties in upscaling yields to the Arctic Ocean. For example, in a literature search for DOC yield values from the seven defined regions (Figure 1), we were only able to find a single source from region 5, the Amygema River (V. Gordeev et al., 1996), and many rivers (like the Vizhas, the Indigirka, and the Moroyyakha) are represented only by a single sample taken in late summer, when discharge is comparatively low and DOC concentrations are not at their maxima (Lobbes et al., 2000). This, unfortunately, tends to lead to a systematic underestimation with respect to DOC flux estimates and so such an approach likely results in an extremely conservative estimate. Thus, scaling from data with temporal resolution that encompasses spring freshet like the exercise undertaken here with the Onega and resulting in a high pan-Arctic DOC flux of 45.08 Tg yr^{-1} may set the upper end of the land-ocean DOC flux as it is unclear how representative the Onega truly is of other regions of the pan-Arctic watershed but it is apparent it has a high DOC yield. Conversely, the average DOC yield scaled from the seven regions may represent the lower end with a pan-Arctic DOC flux of 28.11 Tg yr^{-1} due to limited spatial, but especially temporal resolution feeding into this data set that does not capture time periods that exhibit the highest DOC concentrations (i.e., spring freshet). Thus, the real pan-Arctic land-ocean flux likely lies somewhere between 28.11 and 45.08 Tg yr^{-1} and thus considerable uncertainty remains in this flux term.

Fundamentally, this effort highlights uncertainties that remain in the Arctic land-ocean carbon flux term, and naturally any increase in estimated DOC load has implications for Arctic Ocean biogeochemistry and global climate change. It is apparent that northern high-latitude constrained watersheds have much higher yields of DOC than the six major Arctic rivers due to differences in landcover including permafrost coverage and peatland extent (Frey & Smith, 2005; Holmes et al., 2013) but yet there is no clear relationship to allow scaling from metrics such as watershed carbon storage (Table 3; Figure S6 in Supporting Information S1). Thus, the amount of DOC export potentially unaccounted for from smaller northern high-latitude watersheds focusses attention on the importance of extending data collection to more small- and medium-sized Arctic rivers, especially in the context of building accurate global C budgets.

Data Availability Statement

The data presented here are publicly available at https://doi.org/10.26022/IEDA/112343.

References

Amon, R. M. W., Rinehart, A. J., Duan, S., Louchouarn, P., Prokushkin, A., Guggenberger, G., et al. (2012). Dissolved organic matter sources in large Arctic rivers. *Geochimica et Cosmochimica Acta*, *94*, 217–237. https://doi.org/10.1016/J.GCA.2012.07.015

Amon, R. M. W., Budéus, G., & Meon, B. (2003). Dissolved organic carbon distribution and origin in the Nordic Seas: Exchanges with the Arctic Ocean and the North Atlantic. *Journal of Geophysical Research*, *108*(C7), 3221. https://doi.org/10.1029/2002JC001594

Beck, H. E., Zimmermann, N. E., McVicar, T. R., Vergopolan, N., Berg, A., & Wood, E. F. (2018). Present and future Köppen-Geiger climate classification maps at 1-km resolution. *Scientific Data*, *5*(1), 1–12. https://doi.org/10.1038/sdata.2018.214

Behnke, M. I., McClelland, J. W., Tank, S. E., Kellerman, A. M., Holmes, R. M., Haghipour, N., et al. (2021). Pan-Arctic riverine dissolved organic matter: Synchronous molecular stability, shifting sources and subsidies. *Global Biogeochemical Cycles*, *35*(4), e2020GB006871. https://doi.org/10.1029/2020GB006871

Blakney, G. T., Hendrickson, C. L., & Marshall, A. G. (2011). Predator data station: A fast data acquisition system for advanced FT-ICR MS experiments. *International Journal of Mass Spectrometry*, *306*(2–3), 246–252. https://doi.org/10.1016/J.IJMS.2011.03.009

Brittain, J. E., ısli G ıslason, G. M., Ponomarev, V. I., Bogen, J., Brørs, S., Jensen, A. J., et al. (2009). Arctic rivers. In *Rivers of Europe* (pp. 337–379).

Carstea, E. M., Popa, C. L., Baker, A., & Bridgeman, J. (2020). In situ fluorescence measurements of dissolved organic matter: A review. *Science of The Total Environment*, *699*, 134361. https://doi.org/10.1016/J.SCITOTENV.2019.134361

Chupakov, A. V., Pokrovsky, O. S., Moreva, O. Y., Shirokova, L. S., Neverova, N. V., Chupakova, A. A., et al. (2020). High resolution multi-annual riverine fluxes of organic carbon, nutrient and trace element from the largest European Arctic river, Severnaya Dvina. *Chemical Geology*, *538*, 119491. https://doi.org/10.1016/J.CHEMGEO.2020.119491

Connolly, C. T., Cardenas, M. B., Burkart, G. A., Spencer, R. G. M., & McClelland, J. W. (2020). Groundwater as a major source of dissolved organic matter to Arctic coastal waters. *Nature Communications*, *11*(1), 1–8. https://doi.org/10.1038/s41467-020-15250-8

Corilo, Y. (2015). EnviroOrg. Florida State University.

Cory, R. M., & McKnight, D. M. (2005). Fluorescence spectroscopy reveals ubiquitous presence of oxidized and reduced quinones in dissolved organic matter. *Environmental Science and Technology*, *39*(21), 8142–8149. https://doi.org/10.1021/es0506962

Dankers, R., & Middelkoop, H. (2007). River discharge and freshwater runoff to the Barents Sea under present and future climate conditions. *Climatic Change*, *87*(1–2), 131–153. https://doi.org/10.1007/s10584-007-9349-x

Dittmar, T., & Kattner, G. (2003). The biogeochemistry of the river and shelf ecosystem of the Arctic Ocean: A review. *Marine Chemistry*, *83*(3–4), 103–120. https://doi.org/10.1016/s0304-4203(03)00105-1

Dittmar, T., Koch, B., Hertkorn, N., & Kattner, G. (2008). A simple and efficient method for the solid-phase extraction of dissolved organic matter (SPE-DOM) from seawater. *Limnology and Oceanography: Methods*, *6*(6), 230–235. https://doi.org/10.4319/LOM.2008.6.230

Drake, T. W., Wickland, K. P., Spencer, R. G. M., McKnight, D. M., & Striegl, R. G. (2015). Ancient low-molecular-weight organic acids in permafrost fuel rapid carbon dioxide production upon thaw. *Proceedings of the National Academy of Sciences of the United States of America*, *112*(45), 13946–13951. https://doi.org/10.1073/pnas.1511705112

Evans, C. D., Renou-Wilson, F., & Strack, M. (2016). The role of waterborne carbon in the greenhouse gas balance of drained and re-wetted peatlands. *Aquatic Sciences*, *78*(3), 573–590. https://doi.org/10.1007/s00027-015-0447-y

Fabre, C., Sauvage, S., Tananaev, N., Noël, G. E., Teisserenc, R., Probst, J. L., & Pérez, J. M. S. (2019). Assessment of sediment and organic carbon exports into the Arctic ocean: The case of the Yenisei River basin. *Water Research*, *158*, 118–135. https://doi.org/10.1016/J.WATRES.2019.04.018

Fellman, J. B., Hood, E., & Spencer, R. G. M. (2010). Fluorescence spectroscopy opens new windows into dissolved organic matter dynamics in freshwater ecosystems: A review. *Limnology and Oceanography*, *55*(6), 2452–2462. https://doi.org/10.4319/LO.2010.55.6.2452

Frey, K. E., & Smith, L. C. (2005). Amplified carbon release from vast West Siberian peatlands by 2100. *Geophysical Research Letters*, *32*(9), 1–4. https://doi.org/10.1029/2004GL022025

Gordeev, V., Shirshov, P. P., Gordeev, V. V., Martin, J. M., Sidorov, I. S., & Sidorova, M. V. (1996). A reassessment of the Eurasian river input of water, sediment, major elements, and nutrients to the Arctic Ocean Estimation of the trace metals' accumulation mechanisms in bottom sediments of the White Sea View project. *American Journal of Science*, *296*(6), 664–691. https://doi.org/10.2475/ajs.296.6.664

Gordeev, V. V., & Kravchishina, M. D. (2009). River flux of dissolved organic carbon (DOC) and particulate organic carbon (POC) to the Arctic Ocean: What are the consequences of the global changes? In *Influence of climate change on the changing arctic and sub-Arctic conditions* (pp. 145–160).

Helms, J. R., Stubbins, A., Ritchie, J. D., Minor, E. C., Kieber, D. J., & Mopper, K. (2008). Absorption spectral slopes and slope ratios as indicators of molecular weight, source, and photobleaching of chromophoric dissolved organic matter. *Limnology and Oceanography*, *53*(3), 955–969. https://doi.org/10.4319/LO.2008.53.3.0955

Hendrickson, C. L., Quinn, J. P., Kaiser, N. K., Smith, D. F., Blakney, G. T., Chen, T., et al. (2015). 21 Tesla Fourier transform ion cyclotron resonance mass spectrometer: A national resource for ultrahigh resolution mass analysis. *Journal of the American Society for Mass Spectrometry*, *26*(9), 1626–1632. https://doi.org/10.1007/s13361-015-1182-2

Hodgkins, S. B., Tfaily, M. M., Podgorski, D. C., McCalley, C. K., Saleska, S. R., Crill, P. M., et al. (2016). Elemental composition and optical properties reveal changes in dissolved organic matter along a permafrost thaw chronosequence in a subarctic peatland. *Geochimica et Cosmochimica Acta*, *187*, 123–140. https://doi.org/10.1016/j.gca.2016.05.015

Holmes, R. M., Coe, M. T., Fiske, G. J., Gurtovaya, T., McClelland, J. W., Shiklomanov, A. I., et al. (2013). Climate change impacts on the hydrology and biogeochemistry of Arctic rivers. *Climatic Change and Global Warming of Inland Waters*, 1–26. https://doi.org/10.1002/9781118470596.ch1

Holmes, R. M., Mcclelland, J. W., Peterson, B. J., Tank, S. E., Bulygina, E., Eglinton, T. I., et al. (2012). Seasonal and annual fluxes of nutrients and organic matter from large rivers to the Arctic Ocean and surrounding seas. *Estuaries and Coasts*, *35*(2), 369–382. https://doi.org/10.1007/s12237-011-9386-6

Holmes, R. M., Mcclelland, J. W., Raymond, P. A., Frazer, B. B., Peterson, B. J., Stieglitz, M., et al. (2008). Lability of DOC transported by Alaskan rivers to the Arctic Ocean. *Geophysical Research Letters*, *35*(3), L03402. https://doi.org/10.1029/2007GL032837

Hu, C., Muller-Karger, F. E., & Zepp, R. G. (2002). Absorbance, absorption coefficient, and apparent quantum yield: A comment on common ambiguity in the use of these optical concepts. *Limnology and Oceanography*, *47*(4), 1261–1267. https://doi.org/10.4319/LO.2002.47.4.1261

Hugelius, G., Strauss, J., Zubrzycki, S., Harden, J. W., Schuur, E. A. G., Ping, C.-L., et al. (2014). Estimated stocks of circumpolar permafrost carbon with quantified uncertainty ranges and identified data gaps. *Biogeosciences*, *11*(23), 6573–6593. https://doi.org/10.5194/bg-11-6573-2014

Huguet, A., Vacher, L., Relexans, S., Saubusse, S., Froidefond, J. M., & Parlanti, E. (2009). Properties of fluorescent dissolved organic matter in the Gironde Estuary. *Organic Geochemistry*, *40*(6), 706–719. https://doi.org/10.1016/J.ORGGEOCHEM.2009.03.002

Inamdar, S. P., O'Leary, N., Mitchell, M. J., & Riley, J. T. (2006). The impact of storm events on solute exports from a glaciated forested watershed in western New York, USA. *Hydrological Processes*, *20*(16), 3423–3439. https://doi.org/10.1002/HYP.6141

Johnston, S. E., Carey, J. C., Kellerman, A., Podgorski, D. C., Gewirtzman, J., & Spencer, R. G. M. (2021). Controls on riverine dissolved organic matter composition across an arctic-boreal latitudinal gradient. *Journal of Geophysical Research: Biogeosciences*, *126*(9), e2020JG005988. https://doi.org/10.1029/2020JG005988

Johnston, S. E., Shorina, N., Bulygina, E., Vorobjeva, T., Chupakova, A., Klimov, S. I., et al. (2018). Flux and seasonality of dissolved organic matter from the Northern Dvina (Severnaya Dvina) River, Russia. *Journal of Geophysical Research: Biogeosciences*, *123*(3), 1041–1056. https://doi.org/10.1002/2017JG004337

Kaiser, K., Benner, R., & Amon, R. M. W. (2017). The fate of terrigenous dissolved organic carbon on the Eurasian shelves and export to the North Atlantic. *Journal of Geophysical Research: Oceans*, *122*(1), 4–22. https://doi.org/10.1002/2016JC012380

Kellerman, A. M., Kothawala, D. N., Dittmar, T., & Tranvik, L. J. (2015). Persistence of dissolved organic matter in lakes related to its molecular characteristics. *Nature Geoscience*, *8*(6), 454–457. https://doi.org/10.1038/NGEO2440

Kellerman, A. M., Ois Guillemette, F., Podgorski, D. C., Aiken, G. R., Butler, K. D., & Spencer, R. G. M. (2018). Unifying concepts linking dissolved organic matter composition to persistence in aquatic ecosystems. *Environmental Science & Technology*, *52*(5), 2538–2548. https://doi.org/10.1021/acs.est.7b05513

Koch, B. P., & Dittmar, T. (2006). From mass to structure: An aromaticity index for high-resolution mass data of natural organic matter. *Rapid Communications in Mass Spectrometry*, *20*(5), 926–932. https://doi.org/10.1002/RCM.2386

Kort, E. A., Wofsy, S. C., Daube, B. C., Diao, M., Elkins, J. W., Gao, R. S., et al. (2012). Atmospheric observations of Arctic Ocean methane emissions up to 82° north. *Nature Geoscience*, *5*(5), 318–321. https://doi.org/10.1038/ngeo1452

Kurek, M. R., Poulin, B. A., Mckenna, A. M., & Spencer, R. G. M. (2020). Deciphering dissolved organic matter: Ionization, dopant, and fragmentation insights via Fourier transform-ion cyclotron resonance mass spectrometry. *Environmental Science & Technology*, *54*(24), 16249–16259. https://doi.org/10.1021/acs.est.0c05206

Kurek, M. R., Stubbins, A., Drake, T. W., Moura, J. M. S., Holmes, R. M., Osterholz, H., et al. (2021). Drivers of organic molecular signatures in the Amazon River. *Global Biogeochemical Cycles*, *35*(6), e2021GB006938. https://doi.org/10.1029/2021GB006938

Lambert, T., Bouillon, S., Darchambeau, F., Massicotte, P., & Borges, A. V. (2016). Shift in the chemical composition of dissolved organic matter in the Congo River network. *Biogeosciences*, *13*(18), 5405–5420. https://doi.org/10.5194/BG-13-5405-2016

Lammers, R. B., Shiklomanov, A. I., Vörösmarty, C. J., Fekete, B. M., & Peterson, B. J. (2001). Assessment of contemporary Arctic river runoff based on observational discharge records. *Journal of Geophysical Research*, *106*(D4), 3321–3334. https://doi.org/10.1029/2000JD900444

Lechtenfeld, O. J., Kattner, G., Flerus, R., Mccallister, S. L., Schmitt-Kopplin, P., & Koch, B. P. (2014). Molecular transformation and degradation of refractory dissolved organic matter in the Atlantic and Southern Ocean. *Geochimica et Cosmochimica Acta*, *126*, 321–337. https://doi.org/10.1016/j.gca.2013.11.009

Leech, D. M., ScottEnsign, H., & MichaelPiehler, F. (2016). Spatiotemporal patterns in the export of dissolved organic carbon and chromophoric dissolved organic matter from a coastal, blackwater river. *Aquatic Sciences*, *78*(4), 823–836. https://doi.org/10.1007/s00027-016-0474-3

Lin, H., Xu, H., Cai, Y., Belzile, C., Macdonald, R. W., & Guo, L. (2021). Dynamic changes in size-fractionated dissolved organic matter composition in a seasonally ice-covered Arctic River. *Limnology and Oceanography*, *66*(8), 3085–3099. https://doi.org/10.1002/LNO.11862

Li Yung Lung, J. Y., Tank, S. E., Spence, C., Yang, D., Bonsal, B., McClelland, J. W., & Holmes, R. M. (2018). Seasonal and geographic variation in dissolved carbon biogeochemistry of rivers draining to the Canadian Arctic Ocean and Hudson Bay. *Journal of Geophysical Research: Biogeosciences*, *123*(10), 3371–3386. https://doi.org/10.1029/2018JG004659

Lobbes, J. M., Fitznar, H. P., & Kattner, G. (2000). Biogeochemical characteristics of dissolved and particulate organic matter in Russian rivers entering the Arctic Ocean. *Geochimica et Cosmochimica Acta*, *64*(17), 2973–2983. https://doi.org/10.1016/S0016-7037(00)00409-9

Mann, P. J., Davydova, A., Zimov, N., Spencer, R. G. M., Davydov, S., Bulygina, E., et al. (2012). Controls on the composition and lability of dissolved organic matter in Siberia's Kolyma River basin. *Journal of Geophysical Research*, *117*(G1), 1028. https://doi.org/10.1029/2011JG001798

Mann, P. J., Spencer, R. G. M., Hernes, P. J., Six, J., Aiken, G. R., Tank, S. E., et al. (2016). Pan-Arctic trends in terrestrial dissolved organic matter from optical measurements. *Frontiers in Earth Science*, *4*, 25. https://doi.org/10.3389/FEART.2016.00025

McClelland, J. W., Holmes, R. M., Dunton, K. H., & Macdonald, R. W. (2012). The Arctic ocean estuary. *Estuaries and Coasts*, *35*(2), 353–368. https://doi.org/10.1007/s12237-010-9357-3

McClelland, J. W., Tank, S. E., Spencer, R. G., & Shiklomanov, A. I. (2015). Coordination and sustainability of river observing activities in the Arctic. *The Arctic Observing Summit*, *68*(5), 59–68. https://doi.org/10.14430/arctic4448

McClelland, J. W., Townsend-Small, A., Holmes, R. M., Pan, F., Stieglitz, M., Khosh, M., & Peterson, B. J. (2014). River export of nutrients and organic matter from the North Slope of Alaska to the Beaufort Sea. *Water Resources Research*, *50*(2), 1823–1839. https://doi.org/10.1002/2013WR014722

McKnight, D. M., Boyer, E. W., Westerhoff, P. K., Doran, P. T., Kulbe, T., & Andersen, D. T. (2001). Spectrofluorometric characterization of dissolved organic matter for indication of precursor organic material and aromaticity. *Limnology and Oceanography*, *46*(1), 38–48. https://doi.org/10.4319/LO.2001.46.1.0038

Murphy, K. R., Stedmon, C. A., Graeber, D., & Bro, R. (2013). TUTORIAL REVIEW Kathleen R. Murphy et al. Fluorescence spectroscopy and multi-way techniques: PARAFAC. *Analytical Methods*, *5*(23), 23–24. https://doi.org/10.1039/c3ay41160e

Mutschlecner, A. E., Guerard, J. J., Jones, J. B., & Harms, T. K. (2018). Regional and intra-annual stability of dissolved organic matter composition and biolability in high-latitude Alaskan rivers. *Limnology and Oceanography*, *63*(4), 1605–1621. https://doi.org/10.1002/LNO.10795

O'Donnell, J. A., Aiken, G. R., Swanson, D. K., Panda, S., Butler, K. D., & Baltensperger, A. P. (2016). Dissolved organic matter composition of Arctic rivers: Linking permafrost and parent material to riverine carbon. *Global Biogeochemical Cycles*, *30*(12), 1811–1826. https://doi.org/10.1002/2016GB005482

Ohno, T. (2002). Fluorescence inner-filtering correction for determining the humification index of dissolved organic matter. *Environmental Science and Technology*, *36*(4), 742–746. https://doi.org/10.1021/ES0155276

Oksanen, J., Blanchet, F. G., Friendly, M., Kindt, R., Legendre, P., Mcglinn, D., et al. (2020). Package "vegan" title community ecology package version 2.5-7.

Olefeldt, D., Roulet, N., Giesler, R., & Persson, A. (2013). Total waterborne carbon export and DOC composition from ten nested subarctic peatland catchments—Importance of peatland cover, groundwater influence, and inter-annual variability of precipitation patterns. *Hydrological Processes*, *27*(16), 2280–2294. https://doi.org/10.1002/HYP.9358

Palmtag, J., Obu, J., Kuhry, P., Richter, A., Siewert, M. B., Weiss, N., et al. (2022). A high spatial resolution soil carbon and nitrogen dataset for the northern permafrost region based on circumpolar land cover upscaling. *Earth System Science Data*, *14*(9), 4095–4110. https://doi.org/10.5194/ESSD-14-4095-2022

Parlanti, E., Wörz, K., Geoffroy, L., & Lamotte, M. (2000). Dissolved organic matter fluorescence spectroscopy as a tool to estimate biological activity in a coastal zone submitted to anthropogenic inputs. *Organic Geochemistry*, *31*(12), 1765–1781. https://doi.org/10.1016/S0146-6380(00)00124-8

Peuravuori, J., & Pihlaja, K. (1997). Molecular size distribution and spectroscopic properties of aquatic humic substances. *Analytica Chimica Acta*, *337*(2), 133–149. https://doi.org/10.1016/S0003-2670(96)00412-6

Pokrovsky, O. S., Manasypov, R. M., Kopysov, S. G., Krickov, I. V., Shirokova, L. S., Loiko, S. V., et al. (2020). Impact of permafrost thaw and climate warming on riverine export fluxes of carbon, nutrients and metals in Western Siberia. *Water*, *12*(6), 1817. https://doi.org/10.3390/W12061817

Prowse, T. D., Wrona, F. J., Reist, J. D., Hobbie, J. E., Lévesque, L. M. J., & Vincent, W. F. (2006). General features of the Arctic relevant to climate change in freshwater ecosystems. *Ambio*, *35*(7), 330–338. https://doi.org/10.1579/0044-7447(2006)35[330:gfotar]2.0.co;2

Pugach, S. P., Pipko, I. I., Shakhova, N. E., Shirshin, E. A., Perminova, I. V., Gustafsson, Ö., et al. (2018). Dissolved organic matter and its optical characteristics in the Laptev and East Siberian seas: Spatial distribution and interannual variability (2003–2011). *Ocean Science*, *14*(1), 87–103. https://doi.org/10.5194/os-14-87-2018

Rawlins, M. A., Connolly, C. T., & McClelland, J. W. (2021). Modeling terrestrial dissolved organic carbon loading to western Arctic rivers. *Journal of Geophysical Research: Biogeosciences*, *126*(10), e2021JG006420. https://doi.org/10.1029/2021JG006420

Rawlins, M. A., Steele, M., Holland, M. M., Adam, J. C., Cherry, J. E., Francis, J. A., et al. (2010). Analysis of the Arctic system for freshwater cycle intensification: Observations and expectations. *Journal of Climate*, *23*(21), 5715–5737. https://doi.org/10.1175/2010JCLI3421.1

Raymond, P. A., McClelland, J. W., Holmes, R. M., Zhulidov, A. V., Mull, K., Peterson, B. J., et al. (2007). Flux and age of dissolved organic carbon exported to the Arctic Ocean: A carbon isotopic study of the five largest arctic rivers. *Global Biogeochemical Cycles*, *21*(4). https://doi.org/10.1029/2007GB002934

Raymond, P. A., & Saiers, J. E. (2010). Event controlled DOC export from forested watersheds. *Biogeochemistry*, *100*(1), 197–209. https://doi.org/10.1007/s10533-010-9416-7

Roth, H. K., Borch, T., Young, R. B., Bahureksa, W., Blakney, G. T., Nelson, A. R., et al. (2022). Enhanced speciation of pyrogenic organic matter from wildfires enabled by 21 T FT-ICR mass spectrometry. *Analytical Chemistry*, *94*(6), 2973–2980. https://doi.org/10.1021/acs.analchem.1c05018

Runkel, R. L., Crawford, C. G., & Cohn, T. A. (2004). Load estimator (LOADEST): A FORTRAN program for estimating constituent loads in streams and rivers. *Techniques and Methods*. https://doi.org/10.3133/TM4A5

Savory, J. J., Kaiser, N. K., Mckenna, A. M., Xian, F., Blakney, G. T., Rodgers, R. P., et al. (2011). Parts-per-billion Fourier transform ion cyclotron resonance mass measurement accuracy with a "Walking" calibration equation. *Analytical Chemistry*, *83*(5), 59–1736. https://doi.org/10.1021/ac102943z

Schuur, E. A. G., McGuire, A. D., Schädel, C., Grosse, G., Harden, J. W., Hayes, D. J., et al. (2015). Climate change and the permafrost carbon feedback. *Nature*, *520*(7546), 171–179. https://doi.org/10.1038/nature14338

Selvam, B. P., Lapierre, J. F., Guillemette, F., Voigt, C., Lamprecht, R. E., Biasi, C., et al. (2017). Degradation potentials of dissolved organic carbon (DOC) from thawed permafrost peat. *Scientific Reports*, *7*(1), 1–9. https://doi.org/10.1038/srep45811

Shogren, A. J., Zarnetske, J. P., Abbott, B. W., Iannucci, F., & Bowden, W. B. (2020). We cannot shrug off the shoulder seasons: Addressing knowledge and data gaps in an Arctic headwater. *Environmental Research Letters*, *15*(10), 104027. https://doi.org/10.1088/1748-9326/AB9D3C

Smith, D. F., Podgorski, D. C., Rodgers, R. P., Blakney, G. T., & Hendrickson, C. L. (2018). 21 Tesla FT-ICR mass spectrometer for ultrahigh-resolution analysis of complex organic mixtures. *Analytical Chemistry*, *90*(3), 2041–2047. https://doi.org/10.1021/acs.analchem.7b04159

Speetjens, N. J., Tanski, G., Martin, V., Wagner, J., Richter, A., Hugelius, G., et al. (2022). Dissolved organic matter characterization in soils and streams in a small coastal low-Arctic catchment. *Biogeosciences*, *19*(12), 3073–3097. https://doi.org/10.5194/bg-19-3073-2022

Spencer, R. G. M., Aiken, G. R., Butler, K. D., Dornblaser, M. M., Striegl, R. G., & Hernes, P. J. (2009). Utilizing chromophoric dissolved organic matter measurements to derive export and reactivity of dissolved organic carbon exported to the Arctic Ocean: A case study of the Yukon River, Alaska. *Geophysical Research Letters*, *36*(6), L06401. https://doi.org/10.1029/2008GL036831

Spencer, R. G. M., Aiken, G. R., Dornblaser, M. M., Butler, K. D., Holmes, R. M., Fiske, G., et al. (2013). Chromophoric dissolved organic matter export from U.S. rivers. *Geophysical Research Letters*, *40*(8), 1575–1579. https://doi.org/10.1002/GRL.50357

Spencer, R. G. M., Aiken, G. R., Wickland, K. P., Striegl, R. G., & Hernes, P. J. (2008). Seasonal and spatial variability in dissolved organic matter quantity and composition from the Yukon River basin, Alaska. *Global Biogeochemical Cycles*, *22*(4). https://doi.org/10.1029/2008GB003231

Spencer, R. G. M., Butler, K. D., & Aiken, G. R. (2012). Dissolved organic carbon and chromophoric dissolved organic matter properties of rivers in the USA. *Journal of Geophysical Research*, *117*(G3), 3001. https://doi.org/10.1029/2011JG001928

Spencer, R. G. M., Guo, W., Raymond, P. A., Dittmar, T., Hood, E., Fellman, J., & Stubbins, A. (2014). Source and biolability of ancient dissolved organic matter in glacier and lake ecosystems on the Tibetan Plateau. *Geochimica et Cosmochimica Acta*, *142*, 64–74. https://doi.org/10.1016/j.gca.2014.08.006

Spencer, R. G. M., Hernes, P. J., Ruf, R., Baker, A., Dyda, R. Y., Stubbins, A., & Six, J. (2010). Temporal controls on dissolved organic matter and lignin biogeochemistry in a pristine tropical river, Democratic Republic of Congo. *Journal of Geophysical Research*, *115*(G3), 3013. https://doi.org/10.1029/2009JG001180

Spencer, R. G. M., Kellerman, A. M., Podgorski, D. C., Macedo, M. N., Jankowski, K. J., Nunes, D., & Neill, C. (2019). Identifying the molecular signatures of agricultural expansion in Amazonian headwater streams. *Journal of Geophysical Research: Biogeosciences*, *124*(6), 1637–1650. https://doi.org/10.1029/2018JG004910

Spencer, R. G. M., Mann, P. J., Dittmar, T., Eglinton, T. I., McIntyre, C., Holmes, R. M., et al. (2015). Detecting the signature of permafrost thaw in Arctic rivers. *Geophysical Research Letters*, *42*(8), 2830–2835. https://doi.org/10.1002/2015GL063498

Spencer, R. G. M., Pellerin, B. A., Bergamaschi, B. A., Downing, B. D., Kraus, T. E. C., Smart, D. R., et al. (2007). Diurnal variability in riverine dissolved organic matter composition determined by in situ optical measurement in the San Joaquin River (California, USA). *Hydrological Processes*, *21*(23), 3181–3189. https://doi.org/10.1002/HYP.6887

Stedmon, C. A., Amon, R. M. W., Rinehart, A. J., & Walker, S. A. (2011). The supply and characteristics of colored dissolved organic matter (CDOM) in the Arctic Ocean: Pan Arctic trends and differences. *Marine Chemistry*, *124*(1–4), 108–118. https://doi.org/10.1016/J.MARCHEM.2010.12.007

Striegl, R. G., Aiken, G. R., Dornblaser, M. M., Raymond, P. A., & Wickland, K. P. (2005). A decrease in discharge-normalized DOC export by the Yukon River during summer through autumn. *Geophysical Research Letters*, *32*(21), 1–4. https://doi.org/10.1029/2005GL024413

Tarnocai, C., Canadell, J. G., Schuur, E. A. G., Kuhry, P., Mazhitova, G., & Zimov, S. (2009). Soil organic carbon pools in the northern circumpolar permafrost region. *Global Biogeochemical Cycles*, *23*(2). https://doi.org/10.1029/2008GB003327

Terhaar, J., Lauerwald, R., Regnier, P., Gruber, N., & Bopp, L. (2021). Around one third of current Arctic Ocean primary production sustained by rivers and coastal erosion. *Nature Communications*, *12*(1), 1–10. https://doi.org/10.1038/s41467-020-20470-z

Textor, S. R., Wickland, K. P., Podgorski, D. C., Johnston, S. E., & Spencer, R. G. M. (2019). Dissolved organic carbon turnover in permafrost-influenced watersheds of interior Alaska: Molecular insights and the priming effect. *Frontiers in Earth Science*, *7*, 275. https://doi.org/10.3389/feart.2019.00275

Wagner, S., Fair, J. H., Matt, S., Hosen, J. D., Raymond, P., Saiers, J., et al. (2019). Molecular hysteresis: Hydrologically driven changes in riverine dissolved organic matter chemistry during a storm event. *Journal of Geophysical Research: Biogeosciences*, *124*(4), 759–774. https://doi.org/10.1029/2018JG004817

Wagner, S., Jaffé, R., Cawley, K., Dittmar, T., & Stubbins, A. (2015). Associations between the molecular and optical properties of dissolved organic matter in the Florida everglades, a model coastal wetland system. *Frontiers in Chemistry*, *3*, 66. https://doi.org/10.3389/FCHEM.2015.00066

Wang, P., Huang, Q., Tang, Q., Chen, X., Yu, J., Pozdniakov, S. P., & Wang, T. (2021). Increasing annual and extreme precipitation in permafrost-dominated Siberia during 1959–2018. *Journal of Hydrology*, *603*, 126865. https://doi.org/10.1016/J.JHYDROL.2021.126865

Weishaar, J. L., Aiken, G. R., Bergamaschi, B. A., Fram, M. S., Fujii, R., & Mopper, K. (2003). Evaluation of specific ultraviolet absorbance as an indicator of the chemical composition and reactivity of dissolved organic carbon. *Environmental Science and Technology*, *37*(20), 4702–4708. https://doi.org/10.1021/ES030360X

Williamson, J. L., Tye, A., Lapworth, D. J., Monteith, D., Sanders, R., Mayor, D. J., et al. (2021). Landscape controls on riverine export of dissolved organic carbon from Great Britain. *Biogeochemistry*, 1–22. https://doi.org/10.1007/s10533-021-00762-2

Xian, F., Hendrickson, C. L., Blakney, G. T., Beu, S. C., & Marshall, A. G. (1998). Fourier transforms in NMR, optical, and mass spectrometry: A user's handbook. *International Journal of Mass Spectrometry and Ion Processes*, *17*(1), 8807–8812. https://doi.org/10.1021/ac101091w

Yu, L., & Zhong, S. (2021). Trends in Arctic seasonal and extreme precipitation in recent decades. *Theoretical and Applied Climatology*, *145*(3–4), 1541–1559. https://doi.org/10.1007/s00704-021-03717-7